frontiers | Frontiers in Soft Matter

TYPE Review
PUBLISHED 07 January 2025
DOI 10.3389/frsfm.2024.1518796

OPEN ACCESS

EDITED BY
Tommy Nylander,
Lund University, Sweden

REVIEWED BY
V. Manjuladevi,
Birla Institute of Technology and Science, India
Luigi Paduano,
University of Naples Federico II, Italy

*CORRESPONDENCE
Ingo Dierking,
ingo.dierking@manchester.ac.uk

RECEIVED 29 October 2024
ACCEPTED 16 December 2024
PUBLISHED 07 January 2025

CITATION
Chen C-H and Dierking I (2025) Nanoparticles in thermotropic and lyotropic liquid crystals. *Front. Soft Matter* 4:1518796.
doi: 10.3389/frsfm.2024.1518796

Nanoparticles in thermotropic and lyotropic liquid crystals

Chung-Hao Chen and Ingo Dierking*

Department of Physics and Astronomy, The University of Manchester, Manchester, United Kingdom

Over the last few decades many applications of liquid crystals have been developed, including the widely employed technology of low-power, flat-panel liquid crystal displays (LCDs), but also sensors, photonic devices and other non-display applications employed in medicine and drug delivery. In recent years, the research trends have shifted in other directions. Nanotechnology and nanoscience have garnered significant attention in liquid crystal research since various nanomaterials or nanoparticles (NPs) can be added directly to the liquid crystalline mesogenic phases. The main idea is to modify the physical properties of liquid crystals or to increase their functionality through the addition of nanomaterials, but also to exploit the self-assembly and spontaneous ordering of LCs into structures or patterns that can be templated by dispersed particles. The neat liquid crystals and the doped nanoparticles/nanomaterials exhibit different behaviours when mixed together. The nanoparticles can influence the alignment and orientation of liquid crystals, and their interaction with the liquid crystals causes the changes in the optical, electrical, and mechanical characteristics of the composite. At the same time the liquid crystal can affect the ordering, structuring and properties of the nanomaterials, for example by transfer of helical order. In this review, we discuss the effects of nanoparticles dispersed in liquid crystals. Several categories of nanomaterials such as metallic, carbon allotropes, nanorod and nanowires will be introduced, together with particles of additional functionality, like ferroelectricity, semiconductors and quantum dots. The combination of liquid crystals and nanoparticles leads to a wide range of applications and novel technologies.

KEYWORDS

liquid crystal, thermotropic, lyotropic, nanoparticle, hybrid material

1 Introduction

Liquid crystals (LCs) are a stable thermodynamic state of matter between the solid and the liquid phase, also known as mesophases. This mesophase materials exhibit flow behaviour like a liquid as well as the anisotropic physical properties, as they are often observed in crystals (Collings and Hird, 2017; Engels and von Rybinski, 1998). In general, liquid crystals are considered to be viscous, elastic, anisotropic liquids, thermodynamically distinct from the solid and the isotropic liquid. These materials have a molecular arrangement, in the simplest case exhibiting orientational order of rod-like or disc-like molecules, on average along a common direction called the director **n** (Ohzono and Fukuda, 2012). This orientational director can easily be manipulated by applied external forces such as electric or magnetic fields, but also mechanical fields or even optical fields, in order to change the optical and electrical properties (Lee et al., 1998; Chuang et al., 1991).

Typically, there are two general categories of liquid crystal: thermotropic (Kumar and Brock, 2001; Oswald and Pieranski, 2005) and lyotropic (Neto and Salinas, 2005; Petrov, 1999) liquid crystals. Thermotropic LCs exhibit liquid crystalline behaviour when varying temperature. The molecules forming the LC phases have anisotropic shapes, such as rod-like or disk-like. Thermotropic liquid crystal molecules often exhibit a series of different phase transitions with increasing temperature (Olmsted and Goldbart, 1992). As the temperature is increased, a thermotropic liquid crystal usually transforms from a solid crystalline phase to smectic phases (SmC, SmA), with one- (or higher) dimensional positional order in addition to the orientational order along the director. Further heating then often results in the formation of the nematic phase, which solely exhibits orientational order, and finally the isotropic liquid.

On the other hand, lyotropic liquid crystals (LLC) are molecules or anisotropic nanoparticles dispersed in an appropriate isotropic solvent to form a liquid crystalline state when a specific concentration is reached. LLC are often composed by self-assembly of amphiphilic or chromonic molecules, or anisotropic particles, which can be inorganic, minerals, clays, nanorods, nanowires or sheets, but also of biological nature, such as tobacco mosaic viruses (TMV) or cellulose nanocrystals (CNC), dispersed in a solvent, often water. The formation of lyotropic LCs is more complicated than thermotropic LCs since the liquid crystalline state is sensitive to change not only of temperature but also of each component's concentration (Lagerwall and Scalia, 2012). With increasing the concentration, lyotropic amphiphilic LCs usually exhibit various phases. First, the molecules may assemble into spherical or rod-like micelles, then further aggregate to a hexagonal phase (sometimes also cubic phases are observed) and finally a lamellar phase (Dierking and Martins Figueiredo, 2020) before the inverted phases are observed.

Since the 1960s, LCs have attracted intensive attention due to their unique optical properties, especially in the display industry. The application of Liquid Crystal Displays (LCDs) has significantly changed human's lifestyle. Despite the fact that today these displays have matured technologically, liquid crystals still exhibit a tremendous potential in other research fields, for instance sensors, energy conversion, novel optics, telecommunication, composite materials, biomedicine and biotechnology (Lagerwall and Scalia, 2012; Stannarius, 2009; Jakli, 2010; Dellinger and Braun, 2004; Kim Y. H. et al., 2011; Sivakumar et al., 2009; Kularatne et al., 2017; Kumar, 2006; Woltman et al., 2007). In addition, much effort has been invested into nanotechnology and nanoscience on the basis of liquid crystals and their self-organisation. The field of nanotechnology continues to play a major role in both academia and industry due to its ability to create, explore and exploit materials with unique structural characteristics. These materials have a dimension constrained to the colloidal range from nanometres to several hundreds of nanometres. This nanoscale and the related high surface area leads to unique properties that are significantly different from atoms or molecules, as well as bulk materials. Combining the fields of liquid crystals with nanomaterials opens the doors to a wide range of applications and developments for example in switchable photonics, tuneable metamaterials and the like.

Liquid crystals consist of anisotropic molecules that align in a preferred direction. The orientational direction of the director can be controlled and manipulated by external forces, which can be electric, magnetic, or mechanical in nature. The inherent anisotropic orientation of liquid crystals provides an opportunity through synthesis in LC media, self-organisation, or both in combination, to construct well-defined nanoscale structures. When the nanoscale materials are dispersed into liquid crystals, a wealth of interactions between the host and the particles may be observed (Hegmann et al., 2007; Saliba et al., 2013) such as van der Waals interactions, polar interactions, hydrogen bonding or excluded volume interactions. The resulting composite or dispersion exhibits distinct properties that differ from those of the individual components.

In general, there are several prime groups of nanomaterials that have been used as dopants in LCs, (1) metal nanoparticles, (2) carbon allotropes, (3) inorganic nanorods and nanowires, which can also be semiconducting and ferroelectric, and (4) biomaterials. The choice of dispersion material depends on the desired structure-property relation to be modified and the desired functionalities of the nanomaterial-LC composite (Lapanik et al., 2012; Pal et al., 2015; Dierking, 2019; Singh et al., 2014). In this review, we divided the applications and effects of nanomaterial-liquid crystals composites roughly into these different categories for further discussion. Let us now delve into this exciting field of research and explore some of its findings.

2 Motivation

In general, there are three motivations for doping nanomaterials in liquid crystals: (1) use of the particles to enhance the relevant physical properties of the liquid crystalline phases, such as dielectric anisotropy, electric conductivity, birefringence, viscosity and their related electro-optic parameters, for example threshold voltage (V_{th}), required switching fields, or response times. (2) to improve the orientational order and display parameters of liquid crystalline materials. Here, substrate coatings by nanomaterials can be used to improve LC alignment, produce different device geometries or simply improve the LC order parameter and its physical parameters related to the latter. These aspects are also closely related to the use of liquid crystals in sensors. (3) to enhance the stability of individual phases, tailor the phase transition temperature in phase change processes, or influence the phase sequence. Novel, often frustrated phases can be induced through the dispersion of nanomaterials; already existing phases can be extended and stabilised, for example Blue Phases and other frustrated phases.

When nanomaterials are introduced into a liquid crystal system, the new materials are expected to show different behaviour from the individual components (pristine liquid crystals and nanomaterials) (Goodby, 2011; Poulin et al., 1997; Lehmann et al., 2001; Dierking, 2018; Yu et al., 2016; Garbovskiy and Glushchenko, 2010). The incorporation of nanomaterials into liquid crystals leads to changes in their properties. The nanomaterials influence the parameters that give rise to thermal, electro-optical, and dielectric properties (Garbovskiy and Glushchenko, 2010; Shiraishi et al., 2002; Miyama et al., 2004; Manohar et al., 2009; Li et al., 2013; Manepalli et al., 2018). The interaction in the LC-nanomaterial composite alters their alignment and phase behaviour. The presence

of nanomaterials may enhance the phase stability and widen the temperature range of liquid crystalline phases, which has especially been demonstrated for the blue phases (Bukowczan et al., 2021) which are of interest for novel displays based on the Kerr effect and without the need for alignment layers. The stability of the composite LC phase depends on the factors such as their type, size and shape of the nanomaterial and their anisotropic effects. One example of a complex structure is the Blue phases (BPs), which represents a self-assemble cubic defect structure featuring a local double-twist structure. BPs exhibit unique optical properties such as macroscopic optical isotropy or 3D photonic band gaps and attracted interest in optical devices for example optical fibre sensors (Moreira et al., 2004; Cao et al., 2002). A critical parameter that limits the exploitation of Blue phases is the extremely narrow temperature range in which they occur (Coles and Pivnenko, 2005). By doping a Blue phase liquid crystal mixture with spherical gold nanoparticles, the temperature range could be increased from 0.5 to 5 K. The nanoparticles assemble within lattice disclinations, thereby stabilising the Blue phase structure by lowering the free energy of the system (Yoshida et al., 2009). Another example involves the introduction of surface-functionalised semiconducting nanoparticles into liquid crystals mixtures. Increasing the concentration of nanoparticles significantly widens the Blue phase temperature range, resulting in a robust and stabilised Blue phase structure. This phenomena is greatly enhanced when the nanoparticles are strongly attracted to disclination lines (Karatairi et al., 2010). Only at very high concentrations, when all the defects are filled with nanoparticles, is the system destabilised again and the phase regime of the Blue Phase decreases again.

The dispersion of 0-D nanoparticles, 1-D nanorods or nanotubes and 2-D nanoplates can enhance the self-assembly and order of liquid crystals and promote alignment of nanomaterials themselves. In this way, by the transfer of self-organised order, the liquid crystal can assemble and manipulate particles (Musevic et al., 2006). Moreover, liquid crystals can serve as templates during the synthesis of materials (Wang et al., 2020; Bisoyi and Kumar, 2011; Grzelczak et al., 2010). Self-assembly is the autonomous process in which nanoparticles and other components organise into characteristic structures through various interactions (Whitesides and Grzybowski, 2002; Goodby et al., 2008). By introducing patterns of nanoscale particles, the alignment and ordering of liquid crystals can be controlled. Furthermore, the dispersion of nanomaterials alters the self-organised structures of LCs (Hegmann et al., 2007). The characteristics of nanomaterials such as particle size, composition, shape, and morphology can influence the self-organisation of liquid crystals (Gonçalves et al., 2021; Tripathi A. K. et al., 2013). Nanomaterials can have a profound influence on the orientation of liquid crystals, due to their small elastic constants, so that (in contrast to solid state materials) nanoparticle induced deformations extend largely into the director field. Nanoparticles further exhibit a high surface area, which increases the surface interaction with the liquid crystal molecules. The incorporation of nanomaterials into a liquid crystal influences the alignment and ordering of this LC, leading to the potential of orientational control. The orientation of LCs can be aligned by either doping nanoparticles into the bulk LC or by depositing and growing nanostructure on the substrates (Priscilla et al., 2023). In Brochard and Gennes's work (Brochard and De Gennes, 1970), a low concentration of magnetic nanoparticles was dispersed into a liquid crystal to create a magnetic suspension and control the liquid crystal director via external magnetic fields. The system is like a ferrofluid with an anisotropic liquid as carrier fluid. The application of an external magnetic field reoriented the dispersed ferromagnetic particles and the surrounding liquid crystal molecules underwent a change in orientation and alignment via elastic coupling. Such materials were first wrongly called ferromagnetic nematics, while they should rather be seen as ferrofluids with an anisotropic carrier fluid. True ferromagnetic nematics were only recently discovered by Mertelj (Mertelj et al., 2013; Mertelj et al., 2014).

LCs are anisotropic media and characterised by long-range orientational order, making them well-suited for the dispersion of elongated nanoparticles. For instance, when carbon nanotubes are dispersed in a nematic liquid crystal, the interaction between the carbon nanotubes and the LC results in an increased dielectric anisotropy and a slightly enhanced orientational order (Basu and Iannacchione, 2010). The dispersion of single-wall carbon nanotubes in nematic liquid crystal has also been reported to lead to a decrease of the elastic splay constant, and threshold voltage (Singh et al., 2018a). Nanoparticles with anisotropic properties, such as rod-like or colloidal nanoparticles, when dispersed in liquid crystals, induce an amplified nematic orientational coupling (Li et al., 2006a). Additionally, the changes in LC orientation result in texture changes and modified transition temperatures are observed (Pal et al., 2019). Conversely, liquid crystals can also rearrange the orientation of nanomaterials through elastic interactions while reorienting the director field (Yada et al., 2004; Schwartz et al., 2016).

3 Metal nanoparticles in LCs

3.1 Gold, Au nanoparticles

Metal nanoparticles are widely used to tailor the properties of liquid crystals, and in turn, liquid crystals can tune the properties of metal nanoparticles (Qi and Hegmann, 2006; Barmatov et al., 2004; Yoshikawa et al., 2002; Mitov et al., 2002; Müller et al., 2002). Over the past few decades, metal nanoparticles have been extensively employed due to their size-dependent properties, unlike bulk metals. These nanoparticles exhibit quantum confinement of free electrons. When the nanoparticles absorb light at a frequency matching the natural frequency of the collective electron oscillation, the free electrons on the surface oscillate coherently. This collective oscillation of free electrons is known as surface plasmon resonance (SPR). Due to the strong interaction of the incident electro-magnetic field with the free-electron cloud at the nanoparticles surface, this resonance leads to the absorption and scattering of light, resulting in unique optical properties (Myroshnychenko et al., 2008; Choudhary et al., 2014). In most studies concerning metal nanoparticles and LCs, nano gold is commonly used as a dopant. Gold nanoparticles exhibit SPR in the visible region, and gold is chemically inert and resistant to oxidation, which would change the properties of the nanoparticles.

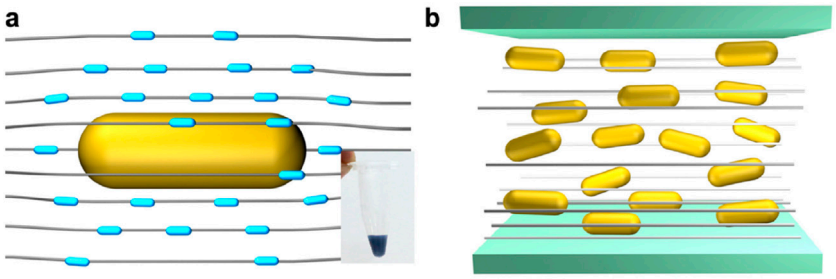

FIGURE 1
(A) Schematic illustration of a gold nanorods with surrounded by rod-like LC molecules depicted in cyan. The inset shows a vial with the gold nanoparticle-5CB dispersion. 5CB is one of the commercially available standard room temperature nematic liquid crystals. **(B)** Schematic of dispersed nanorods following director **n** (Liu et al., 2014a).

The occurrence of SPR in gold nanoparticles enables numerous applications, because the SPR peak can be tuned by changing the size of particle or the dielectric constant of the surrounding medium (Su et al., 2003; Liu et al., 2010). Liquid crystals are particularly suitable as a medium for gold nanoparticle due to the fact that the dielectric constant of LCs can be easily changed through director reorientation by applied external electric fields, reorienting the shape-anisotropic molecules. Gold nanoparticles with SPR can be dispersed within a liquid crystal matrix, offering the potential to harness the unique optical properties of the gold nanoparticles and tune the characteristics of the liquid crystal. When gold nanorods are dispersed in LCs, they can be aligned along the host LC via self-organisation and without external fields applied, thereby allowing for a voltage-controlled tuning of the plasmonic response and the absorption spectra of gold nanorods in liquid crystals (Chu et al., 2006). By applying external magnetic fields or mechanical fields via shear forces, the alignment and reorientation of the liquid crystal may also be achieved, leading to a long-range orientational order of well-dispersed plasmonic nanorods. Consequently, this results in a switchable polarisation-sensitive plasmon resonance that exhibits distinct differences from the behaviour of the nanorods in isotropic fluids (Liu et al., 2010).

Figure 1 illustrates a schematic representation of gold nanorods dispersed in a nematic LC, where the nanorods align with the director field **n(r)** of the host matrix. Orientational order is caused by self-assembly, and the director field is controlled through the LC-surface interactions with the substrates, obtained by unidirectional rubbing. Müller et al., (2002) investigated the surface plasmon splitting of a gold nanoparticle coated with a nematic liquid crystal, finding that the surface plasmon resonance frequency in the scattering cross section depends on the angle between the director and the polarisation of incident light. Later, Park et al. (Park and Stroud, 2004) reported that surface plasmon splitting enables the production of a measurable surface plasmon frequency when the nanorod is oriented in the same direction within the host NLC. However, it was observed that the director field is influenced near the metal surface, and that the surface plasmon splitting is thus reduced (Stark, 2001). When a liquid crystal coated gold nanoparticle is considered, the surface deformation of the liquid crystal can enhance the surface plasmon splitting. Under an applied field, two boojum defects are induced on the surface of the nanoparticle, leading to an enhancement of the peak splitting in the scattering cross section through surface deformation (Park and Stroud, 2005). Liu et al., (2014a) engineered plasmonic guest–host LCs, capable of switching material properties and controlling light propagation across visible and infrared spectral ranges. This involved the controlled dispersion of anisotropic metal nanoparticles in nematic LC [5CB, (4-cyano-4′-pentylbiphenyl)] hosts, enabled by controlled weak anisotropic interactions between the surfaces of nanoparticles and the LC host (Zhang et al., 2015).

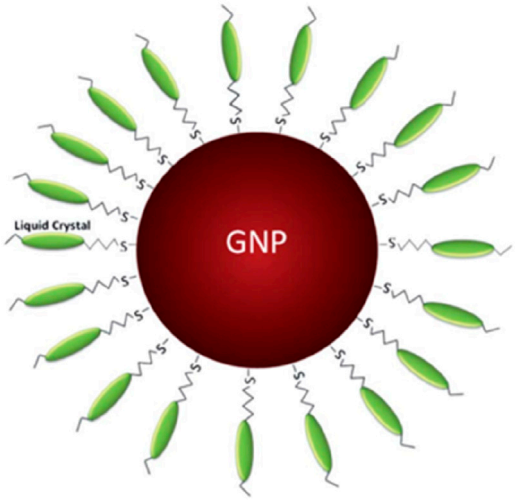

FIGURE 2
Schematic illustration of mesogenic monolayer-capped gold nanoparticle (GNP) (Choudhary et al., 2014).

The gold nanoparticle-liquid crystal composites are typically prepared by dispersing capped nanoparticles (as shown in Figure 2) into an LC in the isotropic phase, followed by ultrasonication over an extended period of time. The capping procedure helps to control the miscibility, prevents agglomeration, and maintains the stability of the composite (Qi et al., 2009; Khatua et al., 2010). Different types of capping using organic/inorganic and biological/inorganic blocks, and the role of the capping in the LC mixture have been discussed (Daniel and Astruc, 2004; Qi and Hegmann, 2011). The solubility of gold nanoparticles is significantly enhanced when the capping material exhibits a chemical structure similar to that of the liquid

crystal molecule. The doping of metallic nanoparticles, such as gold, increases the birefringence of the liquid crystal, and the enhancement of birefringence is influenced by the sizes and concentration of the nanoparticles (Li et al., 2013). Elkhalgi et al. (2018a) investigated the gold nanoparticle-doped nematic liquid crystal 6CHBT composite. They observed the dielectric and electric properties and found that the threshold voltage decreased, while the phase transition (nematic to isotropic) temperature (T_{NI}) and the dielectric permittivity of the composite slightly increased. These effects were attributed to the presence of gold nanoparticles, which increased the nematic order parameter. When gold nanoparticles were dispersed in the nematic LC 5CB, the nematic to isotropic phase transition temperature significantly increased, and the dielectric anisotropy and threshold voltage decreased. Here, the changes were attributed to the formation of anti-parallel dipoles and the availability of extra space for ionic movement in the composite (Pandey et al., 2011), where the anti-parallel dipoles are related to the stability of the nematic phase. Furthermore, when a small concentration of gold nanoparticles (0.02 g solution of 10^{-10} M Au-NPs dispersion) was doped into a polymer-dispersed liquid crystal (E44), the threshold voltage decreased, resulting in a lower switching-on electric fields and the optical transmission was increased (Hinojosa and Sharma, 2010). Also in the case of gold nanoparticles dispersed in ferroelectric liquid crystals (Felix (17/100)), a lower threshold voltage and enhanced optical properties were observed (Kaur et al., 2007). Additionally, a significant enhancement in the photoluminescence intensity was reported by about an order of magnitude (Kumar et al., 2009). A non-volatile memory effect was observed when gold nanoparticles were doped into a deformed helix ferroelectric liquid crystal (DHFLC). This effect is caused by the electric field induce charge transfer from the LC to gold nanoparticles and the stabilisation of helix deformation of LC (Prakash et al., 2008). The charge is stored around the gold nanoparticles and changes the properties of the LC. When a bias field is applied, the cell undergoes a switching mechanism. However, when the bias field is removed, the charges cannot recombine, causing the memory effect.

The electrical conductivity obviously increases by doping gold nanoparticles in the nematic liquid crystals (Prasad et al., 2014; Krishna Prasad et al., 2006), however, the influences on the nematic-isotropic transition temperature of the composite are not consistent. The formation of nanoparticle chains causes the increased conductivity (Holt et al., 2024), reminiscent of a percolation system. Similar phenomena have also been observed with the use of other nano-metals such as silver (Singh et al., 2013), copper (Yaduvanshi et al., 2015) and nickel (Raina, 2013).

The studies mentioned above suggest that nematic LCs are mainly employed to adjust the SPR of gold nanoparticles by tuning the external electric field and temperature conditions. Milette et al. (Milette et al., 2012) reported the formation of structures in high concentrations (5 wt%) of gold nanoparticles dispersed in nematic liquid crystals (5CB). The gold nanoparticles were coated with a mesogenic layer designed to be miscible with the LC (Figure 2). While the mixture was cooled from the isotropic liquid to the nematic liquid crystalline phase, the nanoparticles formed a reversible micron-scale network on cooling across the clearing point by enrichment of the NPs at the nematic-isotropic liquid interfaces (Figure 3). As the film thickness increased to approximately 70 μm, large nematic droplets formed, causing the gold nanoparticles to concentrate in the remaining isotropic liquid region, and resulting in the formation of thick strands. Within each branch, smaller droplets nucleated, as depicted in Figure 3 (d, inset), while the remaining liquid crystal exhibited the nematic Schlieren texture (Figure 3D).

Lyotropic liquid crystals are self-assembled structures composed of amphiphilic molecules or anisotropic particles in combination with an isotropic solvent, often water. Cellulose, an abundant natural biopolymer found in the cell walls of plants, is widely available in nature, making it an inexhaustible material on earth (Brinchi et al., 2013). It is composed of thousands of long chains of sugar units, high molecular weight polysaccharide (Park et al., 2010). Due to the highly ordered structure of cellulose fibres, it can form nanocrystals which in turn assemble to lyotropic liquid crystals when dissolved in suitable solvents, often exhibiting selective reflection, known as Bragg reflection of a wavelength related to the helical pitch of the cholesteric phase (Rojas, 2016). This is particularly of interest when the pitch lies in the visible range.

Cellulose nanocrystals (CNCs) can form lyotropic liquid crystals, in particular helical cholesteric structures, and their incorporation alongside nano gold particles enables the development of functional thin films for applications. The liquid crystal self-organised order of CNCs into a helix acts as a template and provides a structural framework for the dispersed gold particles within the liquid crystal. Gold particles can be adsorbed or bound to the nanocrystals, influencing the morphology and ordering of the mixture. The plasmon properties of nano gold such as surface plasmon resonance (SPR), interact with light to produce enhanced optical responses (Islam et al., 2018). Gold nanorods-CNC composite plasmonic films exhibit strong plasmonic optical activity, which depends on the photonic properties of the CNC host and plasmonic properties of the gold nanorods (Querejeta-Fernández et al., 2014; Liu et al., 2014b). In particular, chiral plasmonic films can be formed. The combination of gold NPs and CNCs provides materials with various applications in optics and sensing. Further investigations involving gold nanoparticles and lyotropic LCs focus on improving optical and electro-optical properties of the dispersions (Shadpour et al., 2019; Liu X. et al., 2019).

3.2 Silver, Ag nanoparticles

Metal nanoparticles are widely and extensively studied because of their exploitable optical properties. Silver (Ag) nanoparticles are one of the popular and widely used variety of metal nanoparticles due to their high electric and thermal conductivity, their chemical stability, the calorimetric effect at nanoscale range and medical application potential (Gittins et al., 2000; Haynes et al., 2003; Crooks et al., 2001). Vimal et al. (Vimal et al., 2017) reported the influence of silver nanoparticles dispersed in ferroelectric liquid crystals (W343). The orientation of nanoparticles in the composite affects the ordering of the LC phase, as shown in Figure 4, the strong repulsive forces between the LC and nanoparticles form the self-assembled 2D-arrays, orientated perpendicular to the rubbing direction, resulting in a modified phase transition, molecular alignment and electro-optics properties.

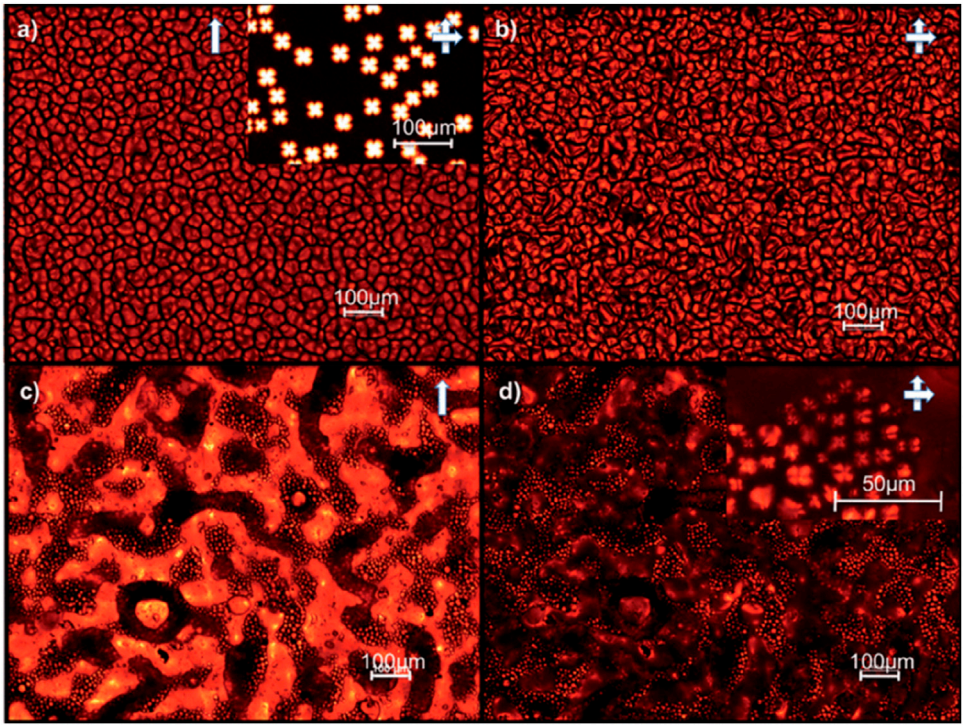

FIGURE 3
POM images of 5 wt% gold nanoparticles dispersed in 5CB. **(A, B)** using untreated 20 µm thick glass cell, resulting in a network of branches and no nodes with Schlieren texture mixed with homeotropically aligned LC. (a, inset) the network starting with nucleating radial nematic droplets. **(C, D)** using untreated 70 µm thick cell, displaying nematic Schlieren texture. (d, inset) A cellular network is formed with stable radial director configuration. **(A, C)** with parallel polarisers, **(B, D)** with crossed polariser (Milette et al., 2012).

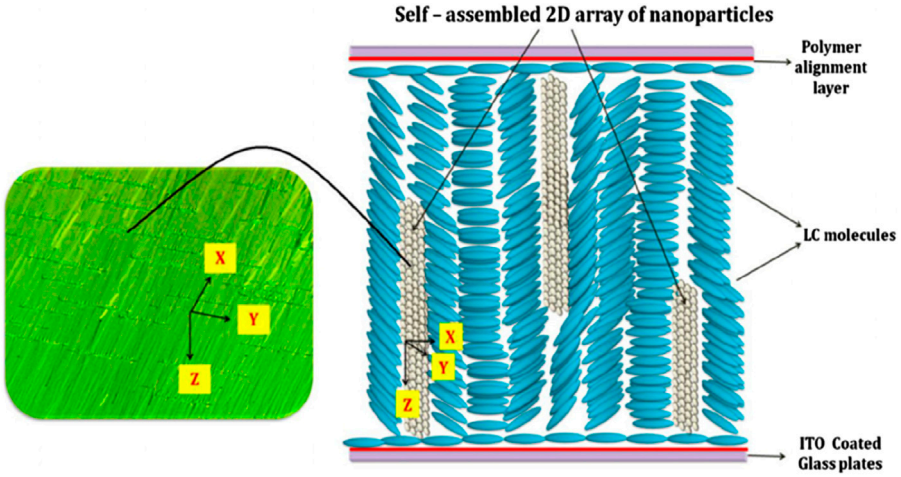

FIGURE 4
Schematic illustration of a cross sectional view from the X-Z plane of the silver nanoparticles dispersed in a ferroelectric smectic liquid crystal system, revealing two-dimensional arrays of nanoparticles between the smectic layers. Disconnecting smectic layers with deformation of layers can be realised due to the 2D array of nanoparticles (Vimal et al., 2017).

When a small amount of Ag (0.02wt% and 0.05wt%) nanoparticles is doped into the nematic LC 6CHBT, some important physical parameters change (Singh et al., 2013). It was thus observed that the threshold volyage decreases, as does the elastic constant. This is most likely due to a decrease in local order in the vicinity of the nanoparticles, due to their boundary conditions, which locally disturbs the far-field orientational order of the nematic, this decreasing the elastic constant which in turn reduces the threshold voltage. The dielectric anisotropy is very slightly reducedby the addition of the nanoparticles, while the

TABLE 1 Effect of metal nanoparticles on the electric properties of liquid crystal.

Metal	Liquid crystals	Results	Ref.
Gold	6CHBT	Vth ↓, TNI ↑, dielectric permittivity ↑	Elkhalgi et al. (2018a)
	5CB	Vth ↓, TNI ↑, dielectric anisotropy ↓	Pandey et al. (2011), Krishna Prasad et al. (2006)
	NLC (PCPBB, HAT6, 5CB)	Electrical conductivity ↑ TNI ↓ for PCPBB, ↑ for HAT6	Prasad et al. (2014), Krishna Prasad et al. (2006), Holt et al. (2024)
	FLC Felix (17/100)	Vth ↓, optical contrast ↑	Kaur et al. (2007)
Silver	6CHBT	Vth ↓, TNI ↑, dielectric anisotropy ↓, elastic constant ↓	Singh et al. (2013), Tripathi et al. (2018)

conductivity anisotropy is substantially increased (Singh et al., 2013). Tripathi et al. also found that the silver nanoparticles decrease the dielectric anisotropy, threshold voltage and elastic constant (Tripathi et al., 2018). Additionally, when CNCs are combined for example with silver nanowires, plasmonic optical activity and a tuneable chiral distribution of aligned silver nanowires with long-range order can be achieved (Chu et al., 2015). Table 1 provides a short summary of liquid crystals doped with metal nanoparticles.

4 Carbon nanoparticles

Another class of nanomaterials that has gained popularity as a dopant in liquid crystals are carbon-based nanomaterials (Clancy et al., 2018; Lisetski et al., 2014; Dolgov et al., 2010; Kumar et al., 2021). Carbon nanomaterials can be categorised into three groups based on their dimensionalities, including fullerenes (0-D), nanotubes (1-D), and graphene derivatives (2-D).

4.1 Fullerenes

Fullerenes are hollow spherical and ellipsoidal molecules composed of 60–70 carbon atoms, arranged in pentagonal and hexagonal patterns. Owing to their unique aesthetic structure and extraordinary properties, fullerenes have generated significant interest (Kroto et al., 1985). The investigation into the dispersion of carbon nanomaterials in liquid crystals began in the early 1990s when Dolganov et al., (1993) first doped the rugby ball-shaped fullerene C70 into a thermotropic liquid crystal, and the polarised absorption spectrum of C70 indicated orientational ordering of the C70 fullerene molecules. Among various fullerenes, C60 has been more frequently and extensively studied. The C60 molecule is a strong electron acceptor, forming corresponding anions, and its molecular structure is spherically symmetric (Li et al., 2012). The studies of fullerenes doped into liquid crystals have primarily focused on enhancing the electrical and electro-optic properties of the composite. The presence of fullerene in liquid crystals changes the photoconductivity, refractive index and dielectric anisotropic properties (Okutan et al., 2005a; Okutan et al., 2005b).

Shukla et al., (2014) reported the dispersion of C60 in a ferroelectric smectic C* liquid crystal and investigated the electro-optical parameters and dielectric responses of the fullerene-FLC composites. As a result, the switching time of the liquid crystal was significantly reduced, showing approximately a 76% increase in speed with a 0.5 wt% of C60. Additionally, the presence of fullerene in liquid crystals can enhance the phase stability of the composite, which is particularly significant for Blue Phases, (BP). One approach to broaden its temperature regime was via polymer-stabilisation (Kikuchi et al., 2002). However, the effectiveness of polymer-stabilisation strongly depends on specific polymer-liquid crystal mixtures, and the consistent observation of BP phase stabilisation remain elusive. Draude et al., (2020) reported the dispersion of a low concentration (0.03 wt%) of C60 in the liquid crystal CE8, which resulted in an expansion of the temperature range of the blue phases from 0.5°C to ~4°C. The width of the chiral nematic phase decreased to accommodate the stabilised blue phase. The small amount of C60 fullerene exhibited a positive impact on the stabilisation of the Blue phase. Since the BP is composed of mutually orthogonal double twist cylinders, which in three-dimensional space cannot be realised without the introduction of defects. These defects form a cubic body- or face-centred lattice at the expense of the free energy. Given their small size, the fullerenes can pack within the space of defects and disclination lines, thus reducing the total free energy of the system. Consequently, the stability of the blue phase is enhanced.

Vovk et al., (2012) reported that a higher concentration of the modified fullerenes (0.1–0.3 wt%) in nematic LC E25M increased electrical conductivity. This is most likely due to residual impurities in the fullerenes, such as metals used during the catalytic synthesis.

Instead of dispersing fullerenes within a liquid crystal phase, it was also demonstrated that fullerenes can be molecularly incorporated into mesogens. In that case the primary application of fullerenes is as a fundamental building block within a mesogenic molecule. In 1996, Chuard and Deschenaux (Chuard and Deschenaux, 1996) first synthesised a molecule containing fullerenes that exhibited thermotropic liquid crystal behaviour. The synthesis was constructed from two cholesterol derivatives bridged through a methano-fullerene structure. The bulky C60 groups hinder the crystallisation.

4.2 Carbon nanotubes

Carbon nanotubes (CNTs) are highly isodiametric, quasi-1D materials with a large aspect ratio (long and thin cylinders), and were discovered in 1991 by Iijima and Ichihashi (Iijima, 1991). CNTs are exist in two basic varieties, which are single-walled carbon nanotubes (SWCNTs) and multi-walled carbon nanotubes (MWCNTs) (Proctor et al., 2017). The former are composed of a single layer hollow cylinder carbon, much like a rolled-up sheet of

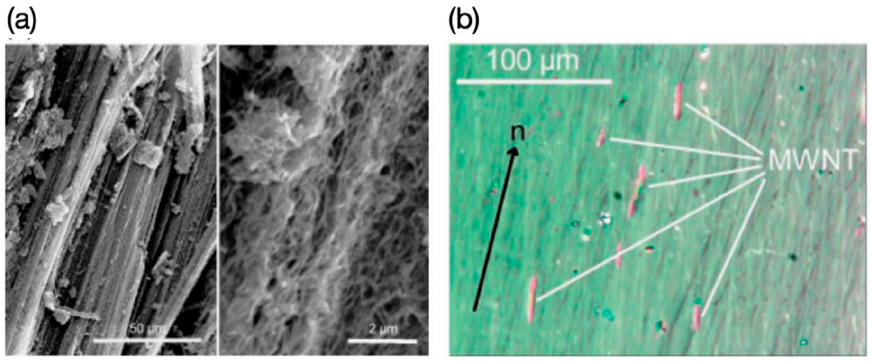

FIGURE 5
(A) SEM images of the employed nanotube materials. MWCNTs aggregate into fibrils (left). These fibrils are not simple carbon fibres; at a larger magnification of 12.7 k (scale bar 2 µm), the individual MWNTs can be resolved (right). **(B)** Polarising microscope image of E7-MWCNT dispersion with MWCNT fibrils oriented along the nematic director (Dierking et al., 2004).

graphene, while the latter are formed by several concentric cylinders. CNTs can have different electronic structures, depending on their configuration, armchair or zigzag and chiral; therefore, they can be semiconductors (MWCNT) or conductors (SWCNT). In the case of conductive nanotubes, the conductivity along the tube axis is much larger than in the radial direction (Reich et al., 2008; Collins and Avouris, 2000). CNTs are highly anisotropic materials and exhibiting a large elastic modulus in direction of the tube axis. The first application of adding carbon nanotubes to liquid crystals was the doping of a thermotropic liquid crystal with multi-walled nanotubes to create diffraction gratings (Lee and Chiu, 2001; Lee et al., 2001). The anisotropic liquid crystal molecules oriented the nanotubes, and then the LC was removed to acquire well-oriented nanotubes (Lynch and Patrick, 2002). In 2004, Dierking et al. (Dierking et al., 2004) reported the behaviour of SWCNTs and MWCNTs dispersed in the nematic liquid crystal E7. In the observation by scanning electron microscopy (SEM), the carbon nanotubes tended to aggregate into larger fibrils, as shown in Figure 5A. After dispersing the single- and multi-walled nanotubes within the liquid crystal, these fibrils further aggregated and aligned along the director of the liquid crystal, as shown in Figure 5B. The nanotubes are mainly oriented along the director, indicating that the orientational order of the LC can be employed to orient the nanotubes on a large scale; the LC director field thus acts like a template for nanotube ordering. Conductivity measurements illustrate a slight increase in the threshold voltage, which is attributed to the interaction between the oriented nanotubes and LC. Above the threshold voltage, the conductivity increased rapidly for the CNT-doped sample due to the spatial reorientation of CNTs following that of the director. These results imply that the LC can not only orient but also reorient carbon nanotubes (Dierking et al., 2005). Figure 6 summarises the reorientation process. Above the threshold voltage, when the applied electric field is active, the LC-CNT dispersion orients into a homeotropic director orientation. The nanotubes follow the liquid crystal director due to elastic interactions and form an oriented conducting percolation network between the two planar electrodes, as shown in Figure 6A. Once the electric field is removed, the LC molecules reorient back to planar orientation due to the cell boundary conditions, resulting in a disruption of the conduction contacts of the nanotube percolation network (Figure 6B). The second reorientation process is attributed to the elastic interaction between the LC and the nanotubes. This elastic interaction causes the nanotube bundles to acquire the orientational order of the LC director field, leading to the reorientation of the nanotubes bundles back to the planar, non-conductive orientation (Dierking et al., 2008). For liquid crystals with negative dielectric anisotropy the reorientation progresses in the opposite way. The CNT doped negatively dielectric nematic under homeotropic boundary conditions shows a strong conductivity, which is largely reduced under electric field application, switching the LC into a planar orientation and the nanotubes following due to elastic interactions. One can thus construct off-on as well as on-off nanotube switches using liquid crystals as a reorientation matrix.

Additionally, instead of using electric field control of the orientation of nanotubes, a magnetically-controlled LC-CNT device has been introduced to manipulate the orientation (Dierking and San, 2005). As the magnetic field reorients the LC from planar to homeotropic alignment, the elastic interaction between LC and CNTs reorients the nanotubes to homeotropic direction above the magnetic threshold field which is in the magnetic case cell gap dependent. In contrast to the electric field, the Freedericksz threshold voltage is independent of the cell gap. However, the threshold magnetic field is inversely proportional to the cell gap.

It has been reported that CNTs dispersed in liquid crystals enhance the electro-optic properties (Shukla et al., 2018; Lee et al., 2004; Baik et al., 2005). Singh et al., (2021) reported the dispersion of MWCNTs increased the permittivity, dielectric anisotropy and enhanced the orientational order of nematic liquid crystals. In the composite of SWCNTs and the nematic LC 3017, there was a decrease in the threshold voltage observed, an enhancement in the nematic ordering of the LC host, and an increase of the dielectric anisotropy. The authors suggested that the interaction between the nanotubes and liquid crystal decreased the splay elastic constant of the dispersed system, causing the decrease in the threshold voltage (Singh et al., 2018b). However, the threshold voltage of CNTs-LC varies with the concentration of nanotubes. With a larger amount of nanotubes (0.5%), the elastic constant of the composite increases

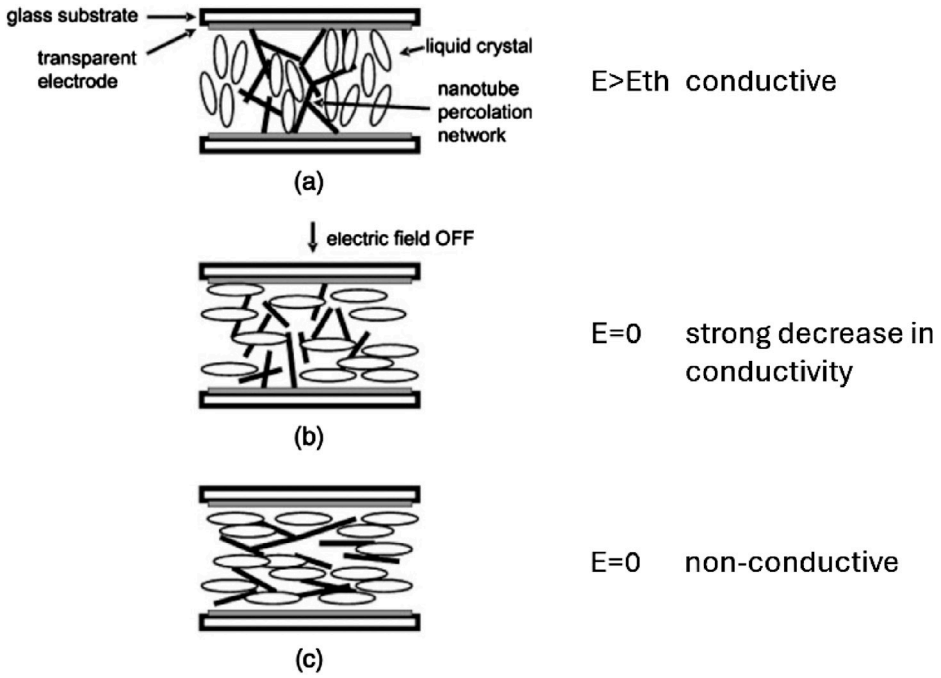

FIGURE 6
A schematic model of the liquid crystal–nanotube dispersion reorientation describing the two-step reorientation process as can be observed in conductivity measurements. **(A)** The initial conductive state where nanotube bundles form a conducting percolation network oriented along the liquid crystal director field. **(B)** Sudden reduction of the electric field below the Freedericksz threshold causes a liquid crystal director reorientation from the homeotropic to the planar state, which in turn disrupts the nanotube percolation network, causing a rapid decrease in conductivity **(C)** Elastic interactions between the nanotube bundles and the liquid crystal matrix cause an orientational reorientation of the nanotube bundles (Dierking et al., 2008).

since the large amount of CNTs cause a compact network aggregate (Ibragimov and Rzayev, 2020). For different LC host materials, the switching behaviour of CNT-LC differs, some results suggesting a decrease of threshold voltage for low nanotube concentrations while an increase could be observed at larger CNT concentrations (Scalia et al., 2007; Schymura and Scalia, 1988). The electro-optic and dielectric properties of carbon nanotubes dispersed in ferroelectric liquid crystals were discussed. Increasing nanotube concentration was found to lead to a decrease in tilt angle yet larger spontaneous polarisation (Yakemseva et al., 2014).

Nanotubes also exhibit a stabilising effect on the Blue Phases. A small amount of SWCNTs doped into CE8 increases the temperature range of the Blue Phase from 0.5 to 4 K (Draude et al., 2020). This increase in phase stability can be explained through a lowering of the free energy density due to nanotubes agglomerating within the Blue Phase defect lattice.

Onsager (1949) described a theory of anisotropic colloids ordering due to the effects of shape by purely repulsive, steric, excluded volume interaction of the dispersed colloids. When the solution concentration exceeds a critical concentration, this leads to a decrease in entropy, causing the anisotropic particles to align and form a liquid crystalline phase. Carbon nanotubes (CNTs) are isodiametric rod-like molecules with a large aspect ratio (long and thin cylinders). DNA modified CNTs (to increase solubility) were shown to exhibit a lyotropic nematic liquid crystal phase when dissolved in an isotropic solvent (Jiang et al., 2007; Song et al., 2003; Bravo-Sanchez et al., 2010; Lu and Chen, 2010; Song and Windle, 2005). Dispersing CNTs in an isotropic solvent is a challenging task, due to their low dispersibility in their natural state. Chemical modification with DNA or in fact covalent bonding of mesogens increases the dispersibility of nanotubes, such that lyotropic liquid crystalline nematic phases have been observed, sometimes also by increasing the CNT concentration via solvent evaporation (Schymura and Scalia, 1988; Jiang et al., 2007; Song et al., 2003).

Song et al. (2003) reported the formation of a lyotropic liquid crystalline phase of MWCNT in water dispersion. The nanotubes were functionalised with -COOH to enhance solubility. The dispersion of nanotubes showed a phase transition from isotropic to lyotropic nematic liquid crystals above the critical concentration. Figure 7A shows the Schlieren texture of nanotubes dispersion at 4.8 vol%. The Schlieren texture contains distinctive “brushes” emanating from topological singularities within the nematic director field. The solvent is dried by evaporating the water, resulting in a solid sample with a microstructure very similar to that of the original dispersion, as shown in Figure 7B. Figures 7C, D illustrate the $s = +1/2$ and $s = -1/2$ defects of the dried structure via scanning electron microscope (SEM) images, where the severe bend distortion close to the core is accommodated by twist distortion between successive layers lying at slightly different depths below the surface. One year later, the authors further studied the isotropic–nematic phase transition in an aqueous dispersion of MWCNTs (Song and Windle, 2005). The polydispersity of CNTs dimensions and straightness influence the coexistence of two phases, the longer and thicker nanotubes are preferentially located in the

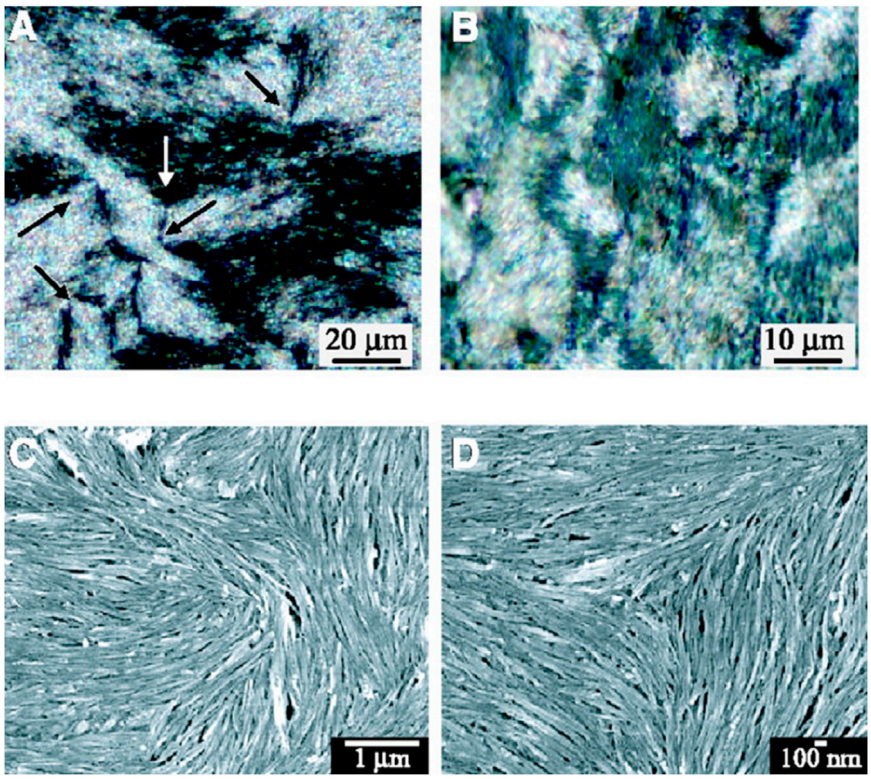

FIGURE 7
(A) Optical image of multiwall carbon nanotubes dispersed in water, showing nematic Schlieren textures. The image is in reflected polarized light with the polars crossed. Singularities at the centre of two-armed brushes correspond to disclinations in the structure. **(B)** Optical image of dried sample **(A)**. Singularities are again indicated by the two-armed brushes. **(C, D)** SEM image of **(C)** a +1/2 topological defect and **(D)** a –1/2 defect from the solid sample of **(B)** (Song et al., 2003).

anisotropic phase. Song and Windle (Song and Windle, 2008) revealed the size dependence of multiwalled carbon nanotube liquid crystalline structures, where longer, straighter nanotubes accumulate in the nematic phase of the dispersion, while short tubes and impurities accumulate in the isotropic liquid.

4.3 Graphene based materials

Another allotrope of carbon, graphene, is one of the most recent carbon allotropes having been discovered. The pioneering research began with Geim and Novoselov (Novoselov et al., 2004), who isolated graphene from graphite. Graphene (GP) is an excellent material for potential technologies due to its properties, such as its large mechanical modulus (Lee et al., 2008) and high electric conductivity (Morozov et al., 2008). Graphene has found wide application potential in a variety of new technologies. Like 1D carbon nanotubes, practically a rolled-up version of graphene, graphene is a 2-dimensional material which exhibits an extremely high aspect ratio, the disk-like structure offers an option to alter the dielectric anisotropic properties of nematic liquid crystals, also changing their threshold voltage, elastic constant and viscosity, when dispersed in a thermotropic LC. Gökçen et al. (2012) reported that the dispersion of 0.05 wt% graphene in nematic liquid crystal E7 significantly increased the threshold voltage from 0.1 V to 1.2 V, and the addition of graphene led to a decrease in polarisation. Wu and Lee, (2013) investigated the phase behaviour and dielectric properties of graphene nanoplatelets dispersed in liquid crystal 8OCB. They found that the transition temperature of nematic to isotropic and smectic A to nematic increased when the graphene nanoplatelets exceeded 0.1wt %. These graphene nanoplatelets enhanced the orientational order of the LC mixture, resulting in an extension of the phase transition temperature. Additionally, the doping of graphene nanoplatelets generated a metastable poly-domain crystalline form, which served as nuclei during crystallisation. In general, liquid crystals doped with graphene show improvements in electro-optic properties such as dielectric anisotropy and faster switching, yet also exhibit an increase in conductivity (Basu et al., 2015; Basu, 2014). Figure 8A shows the increase in dielectric anisotropy when small amounts (0.786×10^{-4} to 3.64×10^{-4} wt%) of graphene are doped into a LC. Figure 8B depicts the electric conductivity for both pure LC (black circles) and the LC-GP composite (green diamonds). Graphene significantly enhances the electric conductivity of the composite when an electric field is applied above the threshold voltage. This is not particularly advantageous for display applications but could be beneficial for other applications like electric liquid crystal switches. The authors (Basu et al., 2015; Basu, 2014) suggested that the increase of the electric conductivity is attributed to the flat surface of graphene being coupled to the director **n** of the LC, i.e. providing internal planar boundary conditions, and reorienting with **n** as the applied field increased, as shown in the scheme. The

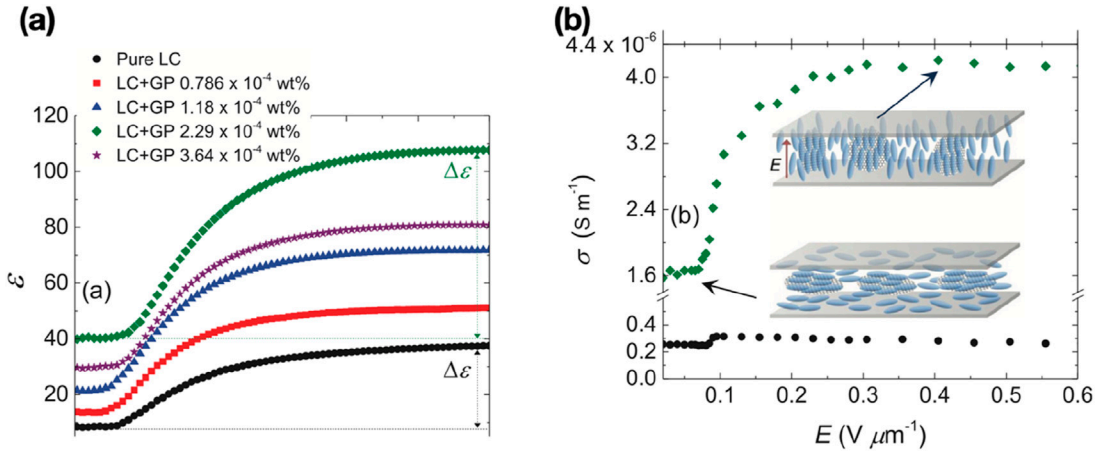

FIGURE 8
(A) Dielectric constant ε as a function of applied rms field in the nematic phase for the pure LC and LC-graphene (LC + GP). **(B)** Electrical conductance σ as a function of applied rms field in the nematic phase for the pure LC and LC + GP 2.29 × 10^{-4} wt%. The reorientation of the graphene flakes with the nematic director is shown in the inset schematics (Basu et al., 2015).

strong π–π electron stacking between the graphene and the LC results in the enhancement of orientation order. However, the solubility and dispersibility of graphene in any solvent or liquid crystal are very poor, limiting its applicational behaviour.

Behabtu et al. (2010) proposed protonated graphene in chlorosulphonic acid exhibited the spontaneous formation of a liquid crystalline phase at high concentrations (20–30 mg/mL). Nevertheless, better materials or solvents need to be found to produce graphene based lyotropic liquid crystals which are easily produced and stable.

Graphene oxide (GO) is such a material, resulting from the decoration of graphene with hydroxy, epoxy and carboxyl groups (Hummers and Offeman, 1958). These functional groups modify the electric properties and raise the amphiphilicity and solubility in solvents. GO retains the mechanical strength and the large aspect ratio of graphene. It is available in large quantities through the chemical oxidation or exfoliation of natural graphite (Stankovich et al., 2006). Al-Zangana et al. (2016a) studied the dispersion of two different sizes of graphene oxide in the nematic liquid crystal 5CB across a wide range of concentrations. They observed that the smaller GO flakes (560 nm) dissolved more easily than larger ones (2.8 μm). Due to the strong surface anchoring of LC molecules on the GO flakes, the dispersions exhibited an increase in both threshold voltage and effective elastic constant. This effect is attributed to the coupling between the liquid crystal and the GO sheets, which strongly increases the effective planar boundary area and thus the threshold voltage. Increasing the GO concentration led to further increases in threshold voltage and elastic constant, reaching saturation at a concentration of about 1 wt%, as shown in Figure 9. The effect was more pronounced for the smaller GO flakes. In the same year, the authors also studied the dielectric behaviour (Al-Zangana et al., 2016b) of dispersed GO of different sizes and concentrations in nematic LC 5CB. The dielectric relaxation of the GO-5CB composite was examined. The GO-LC composite exhibited a dielectric relaxation, while the neat LC did not. This can be explained by the slowing down of the molecular relaxation resulting from the strong anchoring via the GO dispersion interaction.

Javadian et al. (2017) doped graphene oxide into nematic liquid crystal E5CN7. They reported that GO doping led to a significant increase in the nematic-isotropic transition temperature by approximately 12°C, when the concentration of GO reached 0.75 wt%. Özgan et al. (2018) studied the thermal and dielectric properties of GO-doped LC 6CB and found that the dielectric anisotropy of 6CB increased with increasing concentration of GO. Graphene oxide decreased the phase transition temperature approximately by 2 K at 2 wt% doping level. Thermal investigations in general imply that the clearing point of a GO-LC dispersion is strongly dependent on the liquid crystal material used, as well as most likely also on the source of graphene oxide. The threshold voltage generally increases for increasing GO concentration. Additionally, the dielectric anisotropy of 6CB increased with increasing concentration of GO. The change of phase transition temperatures and electro-optical properties resulting from doping GO into a liquid crystal are often not consistent. In 2018, Dalir et al. (2018) reported that GO doping led to an increase in the elastic constant and threshold voltage similar to the observations by Al-Zangana et al. (2016a). Mrukiewicz et al. (2019) again reported a decrease in threshold voltage of 5CB doped with graphene oxide at 0.05–0.3 wt%, with the decrease of threshold voltage being attributed to the disrupted planar alignment caused by the strong interaction between the 5CB's benzene ring and graphene oxide structure. This would imply that the GO sheets do not align with the liquid crystal director. Similar results for GO dispersed in 5CB were reported by Yadav et al. (2020), where the threshold voltage was reported to decrease with the increase in GO concentration (0.04–0.3 wt%) and temperature (26–32°C). The decrease in threshold voltage may be caused by the decrease in orientational order due to the dispersed GO.

Similar to fullerene and carbon nanotubes, graphene oxide dispersed in the Blue Phase also exhibits a stabilisation effect of the latter phase. Doping 0.001 wt% of GO into CE8 increases the temperature range of Blue Phase by 4.3 K. It is presumed that the

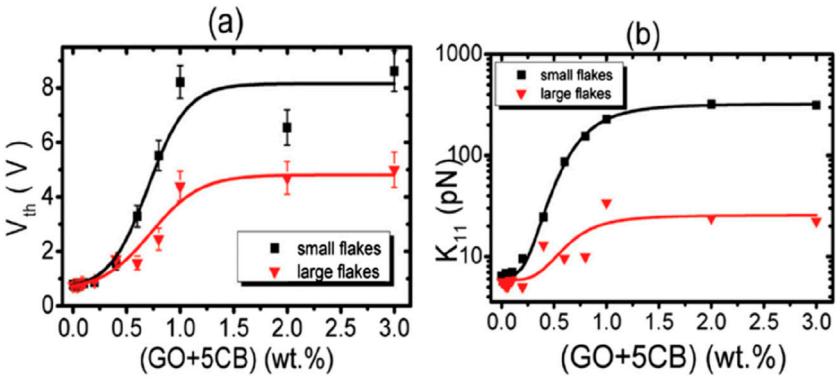

FIGURE 9
(A) Threshold voltage and **(B)** elastic constant as a function of concentration of GO flake in 5CB, for small and large GO sheet sizes (Al-Zangana et al., 2016a).

$\pi - \pi$ stacking between CE8 and graphene oxide stabilises grain boundaries of different Blue Phase lattice orientation, thus leading to a lower free energy and an increased phase stability with the GO accumulating at the grain boundaries (Draude et al., 2020).

Importantly, graphene oxides also exhibit lyotropic liquid crystalline behaviour in a variety of different isotropic solvents, including water. According to Onsager's theory (Onsager, 1949), colloids with a high aspect ratio can self-assemble into a lyotropic liquid crystal phase when a certain concentration range is reached. In 2011, Kim J. E. et al. (2011) first reported that GO in water formed an isotropic-nematic biphasic region in a GO concentration region between 0.05 and 0.7 wt% and a nematic phase above a concentration of approximately 0.6–0.7 wt%, depending on GO source. The orientation of graphene oxide liquid crystals could be manipulated by the application of a magnetic field or through mechanical deformation, i.e. shear. Shen et al. (2014) reported that when the inter-flake interactions are weak, the alignment of GO liquid crystals can be controlled by electric fields, resulting in electro-optic switching due to the Kerr effect. Also in 2011, Xu and Gao (2011a) demonstrated that GO sheets can form a chiral liquid crystal when dispersed in water, in analogy to a twist-grain-boundary (TGB) phase-like model with long-range helical structure and lamellar ordering. At the same time as Kim J. E. et al. (2011), Xu and Gao (2011b) also discussed the aqueous dispersion of single-layered graphene oxide and established the nematic-isotropic phase diagram versus mass fraction. The GO formed a lyotropic LC which exhibiting birefringence between crossed polarisers above a critical concentration. Figure 10A shows the microscopic images of a GO-water dispersion. Above the mass fraction of 5×10^{-3} a uniform birefringent sample was observed which displayed a nematic Schlieren texture. Also, the macroscopic images in test tubes show similar results. With increasing the GO concentration, the textures of the LC could be observed by the naked eye between crossed polarisers, and the birefringence became more colourful, illustrating the formation of the nematic phase, as shown in Figure 10B. Upon increasing the GO concentration further, GO sheets can lead to the formation of a lamellar phase. The aspect ratio of GO sheets influences the stability of liquid crystal formation. For an increasing aspect ratio, the degree of GO with a corrugated morphology in the solvent is enhanced (Li et al., 2014). The high aspect ratio of the GO sheets leads to a lower critical concentration to form a liquid crystal phase (Aboutalebi et al., 2011). The size of GO sheets also influences the lyotropic liquid crystalline phase diagram (Al-Zangana et al., 2017a). Below a certain limit of sheet size (0.27 μm), GO does not form a LC phase. Increasing GO sheet sizes favours lyotropic liquid crystal formation (Aboutalebi et al., 2011; Dan et al., 2011). The solvent also plays an important role in the formation of GO lyotropic LC phases. Solvents with higher dielectric constants or higher relative static permittivity can more easily form LC phase at lower GO concentrations or smaller GO sheet sizes (Al-Zangana et al., 2017a). Jalili et al. (2013) discussed the behaviour of GO dissolved in different organic solvents, and the ability to form LC phase is attributed to the polarity and dielectric constant of the solvents. More discussion on optimising graphene oxide liquid crystal (GOLC) phase formation and different characterisation methods for different types of GOLC phases can be found in the review by Sasikala et al. (2018). The effect of liquid crystals doped with carbon-based nanoparticles are summarised in Table 2.

5 Semiconducting, ferroelectric, and metal oxide particles

Inorganic materials are often dispersed in liquid crystals to tune properties, such as dielectric [TiO_2 (Chen et al., 2009)] or ferroelectric ($BaTiO_3$ (Singh et al., 2014)) particles, metal oxide [V_2O_5 (Diesselhorst and Freundlich, 1915)] and semiconducting particles [CdSe (Li et al., 2002)]. Doping semiconducting or metal oxide particles into liquid crystals can tune electric properties, such as threshold voltage, viscosity, dielectric anisotropy (Chen et al., 2009; Williams et al., 2005; Mukhina et al., 2012; Joshi et al., 2010) and can also stabilised the Blue phase structure (Karatairi et al., 2010). O Dolgov and V Yaroshchuk (2004) reported that the dispersion of silica particles showed electro-optic memory, and the preparation method of nanoparticles strongly effected the electro-optic properties. Tripathi P. K. et al. (2013) doped zinc oxide (ZnO) into nematic LC MBBA, resulting in an increase of the dielectric anisotropy, threshold voltage, elastic constant and viscosity, while the response time was reduced. Similar results

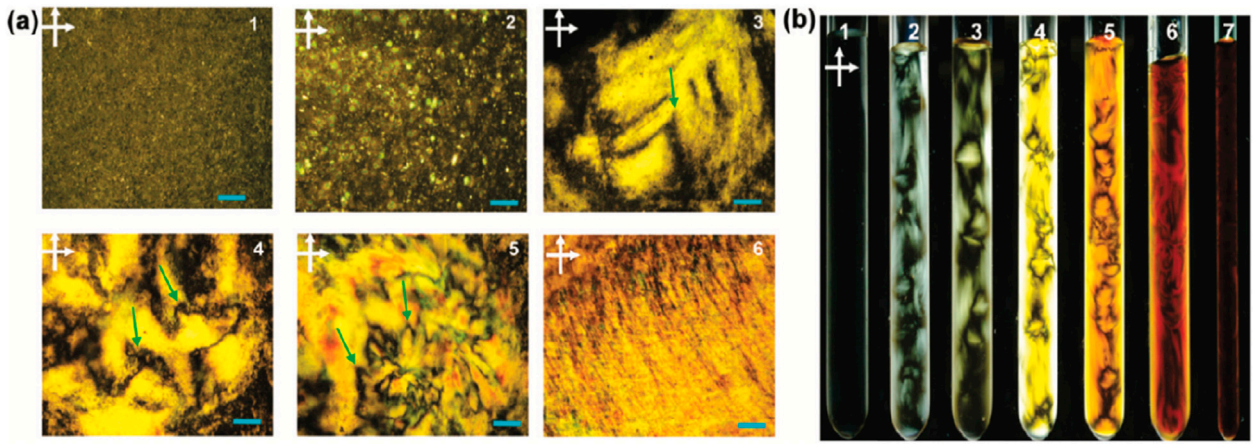

FIGURE 10
(A) POM images between crossed polarizers of GO aqueous dispersions in planar cells with mass fraction of 5×10^{-4}, 1×10^{-3}, 3×10^{-3}, 5×10^{-3}, 8×10^{-3}, and 1×10^{-2} (from 1 to 6). The scale bar represents 200 μm **(B)** Macroscopic photographs between crossed polarizers of GO aqueous dispersions with mass fraction of 1×10^{-4}, 2.5×10^{-4}, 5×10^{-4}, 1×10^{-3}, 5×10^{-3}, 1×10^{-2}, 2×10^{-2}. (from 1 to 7) (Xu and Gao, 2011b).

TABLE 2 Effect of carbon nanoparticles on the electric properties of liquid crystal.

Material	Liquid crystals	Results	Ref.
Fullerene	FLC	Switching time ↓	Shukla et al. (2014)
	CE8	BPs range ↑	Draude et al. (2020)
	E25M	Electric conductivity ↑	Vovk et al. (2012)
Nanotube (SWCNT and MWCNT)	NLC (E7, ZLI2806)	Vth ↑, electric conductivity ↑ Orient the nanotube	Dierking et al. (2004)
MWCNTs	NLC (W-3017)	Permittivity ↑, dielectric anisotropy ↑, orientational order ↑	Singh et al. (2021)
SWCNTs	NLC (3017)	Vth ↓, dielectric anisotropy ↑, elastic constant ↓	Singh et al. (2018b)
	5CB	Vth ↑, elastic constant ↑ when (nanotube 0.5%), switching time ↓	Ibragimov and Rzayev (2020)
	CE8	BPs range ↑	Draude et al. (2020)
Graphene	E7	Vth ↑, polarisation ↓	Gökçen et al. (2012)
	8OCB	TNI ↑, TsmA-N ↑	Wu and Lee (2013)
	MLC-15600–100	Switching time ↓, electric conductivity ↑, dielectric anisotropy ↑	Basu et al. (2015)
Graphene Oxide	5CB	Elastic constant ↑, Vth ↑	Al-Zangana et al. (2016a)
	E5CN7	TNI ↑, elastic constant ↑, Vth ↑	Javadian et al. (2017), Dalir et al. (2018)
	6CB	TNI ↓, dielectric anisotropy ↑, Vth ↑	Özgan et al. (2018)
	5CB	Vth ↓ at GO 0.05–0.3 wt%	Mrukiewicz et al. (2019), Yadav et al. (2020)
	CE8	BPs range ↑	Draude et al. (2020)

were also shown for Fe_2O_3 (Ye et al., 2017) and Manganese titanium oxide ($MnTiO_3$) (Elkhalgi et al., 2018b).

The elasticity and topological defects of the LC host have been utilised to assemble microparticles in various geometries (Blanc et al., 2013; Smalyukh, 2018). When colloids or microparticles are dispersed in a nematic liquid crystal, the local orientation of the LC is determined by the surface interactions, resulting in different self-assembled structures (Musevic et al., 2006; Lapointe et al., 2009; Muševič and Škarabot, 2008). Musevic et al. (2006) demonstrated the dispersion of micrometre-sized silica spherical particles in thin films of nematic liquid crystals forming two dimensional lattice structures. Figure 11 shows a silica sphere in a nematic liquid crystal. When the thickness of the LC layer is above approximately 5 μm, with particles of size 2.3 μm (Figure 11A), the director field around the colloid is distorted into a dipolar shape (Figure 11B), and colloids assemble into chains oriented along the rubbing direction (Figure 11C). Conversely, when the thickness is below approximately 3.5 μm for the same particle size, the director field around the colloid exhibits two dark

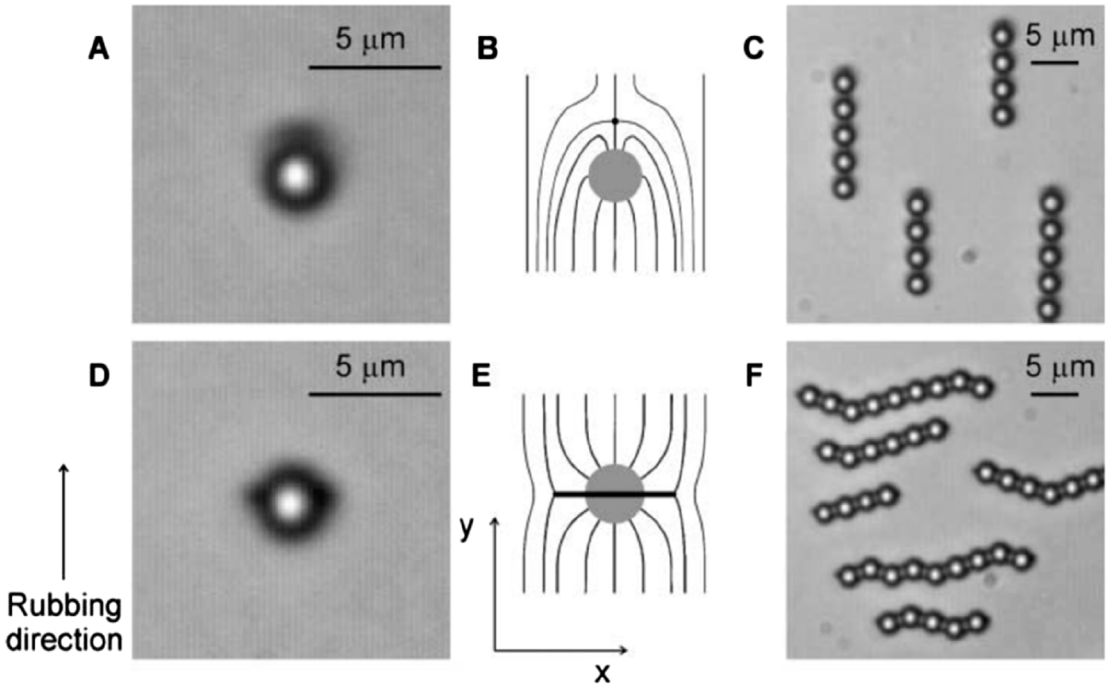

FIGURE 11
Dipolar and quadrupolar colloids in a thin layer of a nematic liquid crystal. **(A)** Micrograph of a d = 2.32 µm silica sphere in 5CB layer with 5 µm thickness. **(B)** Schematic illustration of the nematic order around the colloid has the symmetry of an electric dipole. **(C)** Dipoles form dipolar chains along the rubbing direction. **(D)** Micrograph of a d = 2.32 µm silica sphere in 5CB layer with 2.5 µm thickness. **(E)** Schematic illustration of the nematic order has the symmetry of an electric quadrupole. **(F)** Quadrupoles form kinked chains aligned perpendicular to the rubbing direction (Musevic et al., 2006).

regions between crossed polarisers, representing the Saturn ring defect encircling the colloid. The director field is quadrupolar (Figure 11D), and the colloids are oriented perpendicular to the rubbing direction in a zig-zag fashion (Figure 11F). The structures observed for colloids in a thin nematic layer are spontaneously stable and exhibit long-range orientation.

5.1 Metal oxide particles

One dimensional (1-D) nanostructures such as nanowires and nanorods, have drawn tremendous attention in both fundamental science and technology applications due to their electrical and optical properties (Hu et al., 1999; Lieber, 1998). Unlike nanotubes, which generally exhibit a pronounced polydispersity, nanorods are often closer to the ideal Onsager-like system (Onsager, 1949). Rod-like particles often have orientational order and no positional order, forming nematic liquid crystalline phases, although the formation of smectic phases is known as well. Zinc oxide (ZnO) is most often a white powder that is insoluble in water, often used as an additive in paint. ZnO nanowires are semiconductors with a high aspect ratio. Zhang et al. (2011) reported that ZnO nanowires exhibit liquid crystalline behaviour in aqueous and organic solvents. With an increase in ZnO concentration, the mixture transitions from an isotropic via a biphasic state to a nematic phase, as shown in Figure 12. The alignment of nanowires can be controlled by shear flow; after solvent evaporation, the dried nanowire assembly inherits the alignment of the nematic suspension, as shown in Figure 12F.

Silica nanoparticles were probably some of the first materials to be doped into liquid crystal phases. Dispersion into nematic phases (Yadav et al., 2019) has shown that a very well aligned neat nematic phase experiences disturbances in the director field which slowly degrade the alignment with increasing silica nanoparticle concentration. Nevertheless, an increase in birefringence is observed for increasing concentration. At the same time the relative dielectric permittivity is slightly decreased and at low frequencies the ionic contribution to the dielectric spectra is decreased, which indicates that the ions are possibly adsorbed on the silica particles (Liao S.-W. et al., 2012). The bulk conductivity was found to be increased for increasing silica concentration. The authors further report an enhancement of photoluminescence with a slight redshift for increasing silica concentration, and also an increased UV absorbance.

In Blue Phases (Hsu et al., 2018) the dispersion of silica nanoparticles has been shown to widen the existence range of the BP phase and a decrease in the driving voltage of the electro-optic Kerr effect, combined with a decrease of rise and fall time for increasing concentration.

Dispersing silica into the ferroelectric SmC* phase (Chaudhary et al., 2012) allows a tuning of the electro-optic properties. The tilt angle and thus also the spontaneous polarisation were found to decrease for increasing particle concentration when compared to the pure ferroelectric phase. The rotational viscosity is decreased for increasing concentration, and thus the response time become faster. The dielectric permittivity was reported to be decreased for increasing silica nanoparticle levels. Other reports (Kumar and Raina, 2012)

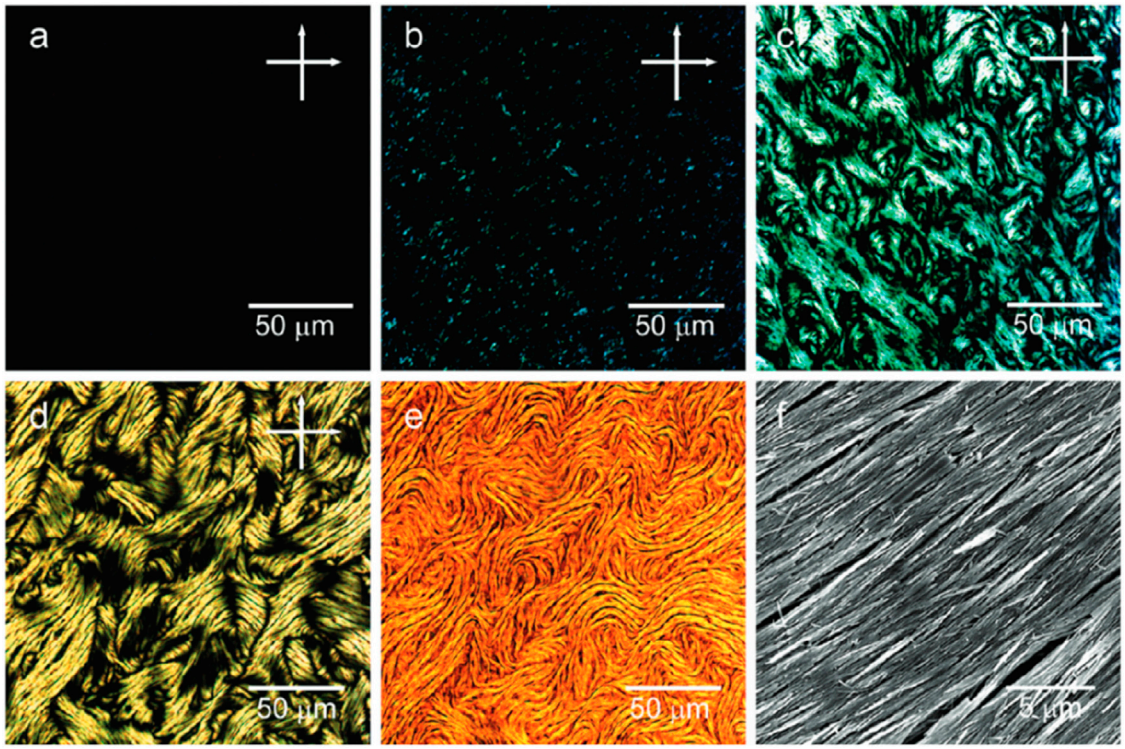

FIGURE 12
POM images of ZnO nanowire in solvent. **(A)** 0.5% ZnO showing the isotropic phase; **(B)** 2.3% ZnO showing biphasic phase **(C)** 6.3% ZnO showing Schlieren texture **(D)** dried nanowire under crossed polariser **(E)** dried nanowire without polarisers **(F)** SEM image of dried long-range oriented nanowire (Zhang et al., 2011).

also indicate a decreasing tilt angle and spontaneous polarisation, but a slightly increasing rotational viscosity and thus an increase in response time with increasing silica nanoparticle concentration. They also found that the contrast ratio was enhanced.

But also more exotic systems have been doped with silica nanoparticles, for example nematic polymer dispersed liquid crystals (PDLC) (Jayoti et al., 2017). The authors reported slightly decreased transition temperatures for increasing silica concentrations, of the order of 2–3 K. The transmission was increased as a function of nanoparticle concentration, while at the same time the threshold voltage and the conductivity were reduced.

From the viewpoint of nanoparticle doping, a particularly unusual study was reported in (Landman et al., 2014). Here, the authors doped a lyotropic nematic clay (beidellite) suspension with silica particles of increasing concentration. They found that the two-phase region not only shifted to higher beidellite concentrations but was also widened. The viscosity of the silica nanoparticle doped clay suspension markedly increased with increasing concentration of silica at constant beidellite concentration.

5.2 Semiconducting nanoparticles

Cadmium selenide nanorods are semiconducting materials. Alivisatos et al. (Li et al., 2002) reported the liquid crystalline phase of CdSe semiconductor nanorods. When the CdSe nanorods are dissolved in cyclohexane at high concentration (>10 wt%), the nematic phase is observed to occur during solvent evaporation (Figure 13A), showing Schlieren textures in polarising optical microscopy, as shown in Figure 13B. The authors suggest that the liquid crystalline phase of CdSe nanorods exhibits a larger elastic constant than regular organic LC molecules due to the size and rigidity of the nanorods. Additionally, CdSe nanorods have shown photoluminescence which is linearly polarised along the long axis (Hu et al., 2001). The liquid crystal formed by CdSe nanorods can be aligned and the director controlled by external electric, magnetic or mechanical fields. One can thus change the polarisation direction of photoluminescence, for example in devices with in-plane electrodes.

One year later, Li and Alivisatos (2003) reported the alignment, orientation, and surface deposition of CdSe nanorods from the lyotropic liquid crystalline phase. The CdSe nanorods are enabled to be synthesised with a well-controlled width (3.0–6.5 nm) and length (7.5–40 nm) (Li et al., 2001). The macroscopic alignment of CdSe nanorods was observed by transmission electron microscopy (TEM). As the solvent evaporated, the CdSe nanorods were deposited, aligned along the nematic director of the self-organised liquid crystal phase it formed during the increase of nanorod concentration in the solvent. By controlling the orientation of the liquid crystal through external fields, a high degree of orientational order of deposited nanorods can be achieved.

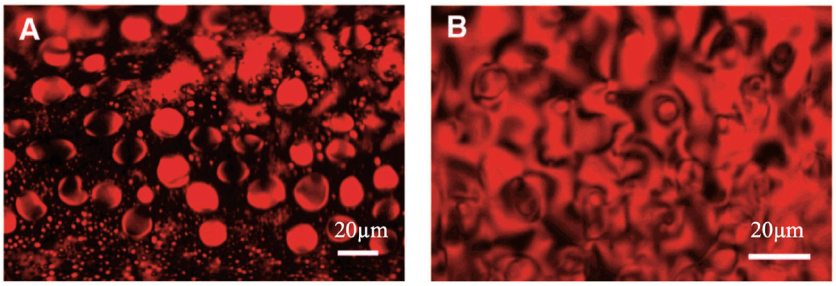

FIGURE 13
POM image CdSe nanorods in cyclohexane during solvent evaporation. **(A)** Nematic droplets formed from the isotropic phase during the evaporation of the solvent. **(B)** Schlieren textures in a later stage, at high CdSe concentration (Li et al., 2002).

5.3 Ferroelectric nanoparticles

Before concluding this section, it is important to introduce ferroelectric particles. Ferroelectricity is a property observed in materials where permanent electric dipoles add to form a non-zero spontaneous polarisation that can be reoriented between two stable states by an externally applied electric field. Ferroelectric liquid crystals (FLC) are a type of liquid crystal that exhibit ferroelectric properties, characterised by the spontaneous polarisation of the sample. FLCs can switch their molecular orientation in response to an electric field and the coupling between electric field and polarisation leads to a fast response in the microsecond regime (Chigrinov, 1999; Chigrinov et al., 2013). The spontaneous polarisation of ferroelectric particles may induce an electrical polarisation within the surrounding LC, leading to an increase in the order parameter of the doped LC and an increase in its clearing temperature (Li et al., 2006a). By doping 0.2 wt% of ferroelectric particles into the LC, the nematic orientational order parameter increased by 10%, and the clearing temperature rose by 40°C. Lopatina and Selinger (2011); Lopatina and Selinger (2009) discussed the mechanics of ferroelectric particles in liquid crystals through a Landau theory, which predicts an increase in the nematic-isotropic temperature and sensitivity to the electric field. Reznikov et al. (2003) reported that a low concentration of nano-sized ferroelectric $Sn_2P_2S_6$ particles in the nematic LC ZLI-4801 enhances the dielectric response and order parameter without disturbing the alignment of LC molecules. Kurochkin et al. (2010) doped ferroelectric nanoparticle $Sn_2P_2S_6$ into 5CB, leading to a shift in the clearing temperature, and the corresponding changes in the order parameter were observed. The dielectric anisotropy and birefringence increased due to the increase of the order parameter. This was explained by Shelestiuk et al. (2011) who developed a theoretical model for the dielectric properties of a LC nanosuspension with ferroelectric particles. It was further predicted that the ferroelectric particles decrease the Freedericksz transition threshold voltage. The latter was demonstrated experimentally by Cîrtoaje et al. (2015) who measured the electric properties of the nematic LC 5CB with shape-anisotropic ferroelectric $BaTiO_3$. The threshold voltage was found to be lower when the ferroelectric particles were added, indicating that the particles are oriented parallel to the LC. When the nanoparticles are perpendicular to the LC molecules, the threshold voltage may increase.

Reznikov and co-workers made a dilute suspension of ferroelectric particles $Sn_2P_2S_6$ suspension in the nematic LC ZLI-4801. The nanoparticles did not disturb the director field of the LC. Simultaneously, due to their anchoring with the LC, the large dipole moment and high polarizability of the ferroelectric particles, the doping increased the dielectric anisotropy, the static dielectric permittivity (Ouskova et al., 2003; Buchnev et al., 2003; Buchnev et al., 2004), and decreased the threshold voltage (Reznikov et al., 2005). In addition, introducing ferroelectric nanoparticles into a cholesteric mixture used in a scattering device decreased the driving voltage from clear to scattering by 45%, which was caused by the increased dielectric anisotropy of the cholesteric mixture. Due to the permanent polarisation of ferroelectric particles, the birefringence increased in both the nematic and the cholesteric liquid crystals (Kurochkin et al., 2009). Another common ferroelectric is the above-mentioned barium titanate ($BaTiO_3$), which has a spontaneous polarisation, depending on the size and fabrication/treatment of the nanoparticles. Doping a low concentration of $BaTiO_3$ significantly increases the phase transition temperature, birefringence, dielectric anisotropy and elastic constant (Li et al., 2006b; Glushchenko et al., 2006). Liang et al. (2010) dispersed $BaTiO_3$ into the ferroelectric liquid crystal (FLC) CS1024, resulting in a spontaneous polarisation of twice that compared to the pure FLC. The response time was shortened, and the dielectric constant was increased, especially for the smectic C* phase. Also the size effect of $BaTiO_3$ has been investigated; Rudzki et al. (2013) dispersed various sizes of $BaTiO_3$ into different FLC mixtures. The smaller particles (9 nm) exhibited more pronounced effects on spontaneous polarisation and switching time than the larger ones (26 nm). This result is somewhat surprising, as it is generally believed that barium titanate at low nanometre dimensions <100 nm exhibits a cubic unit cell and is thus not ferroelectric. Only for larger sizes a tetragonal unit cell is generally observed, together with ferroelectricity for particles of size >100 nm. Nevertheless, it should be pointed out that the crystal structure of barium titanate strongly depends on the method of nanoparticle production, milling etc.

The electro-optic properties of various sizes $BaTiO_3$ in nematic liquid crystals were also measured by Herrington et al. (2010), with larger particles causing a more significant enhancement of dielectric and optical anisotropy. Al-Zangana et al. (2017b) investigated the effects of different sizes and concentrations of barium titanate in the nematic LC 5CB and the ferroelectric SmC* M4851/050. It was

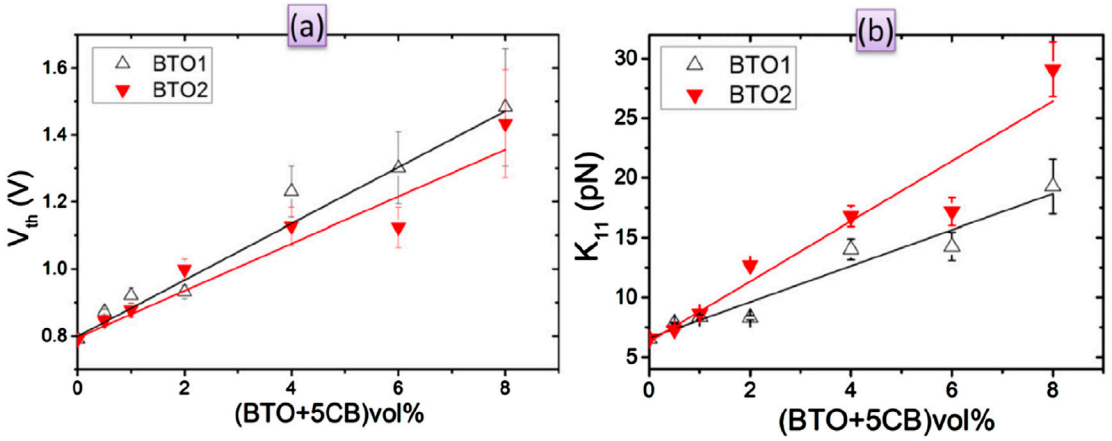

FIGURE 14
The relationship between the concentration of BaTiO3 and **(A)** Threshold voltage and **(B)** elastic constant, where BTO1 (80 nm) and BTO2 (240 nm) are the size of nanoparticles (Al-Zangana et al., 2017b).

found that a low concentration of nanoparticles did not influence the electro-optic properties at all. At higher concentrations, the nanoparticles increased the threshold voltage and elastic constant of the mixture, as shown in Figure 14. However, the ferroelectric particles had no significant effects on the electro-optic properties of a ferroelectric SmC* liquid crystal. The physical properties of the ferroelectric particles dispersion can vary depending on the size, shape, LC host and the method of preparation (Gupta et al., 2010). Cook et al. (2010) and Blach et al. (2010) reported that the dispersion of $BaTiO_3$ decreases the threshold voltage, meanwhile, Glushchenko et al. (2006) and Klein et al. (2013) found that doping ferroelectric particles did not change the threshold voltage significantly. Paul et al. (2011) reported an increase in the threshold voltage due to the dispersion of $BaTiO_3$. Further investigations of electro-optical properties have been carried out (Singh et al., 2014; Podoliak et al., 2014; Coondoo et al., 2011).

The dispersion of ferroelectric particles can modify the electro-optic and polarisation effects and shows the potential for display or electro-optic applications. Yet it appears that the modifications are strongly dependent on size, shape and production of the ferroelectric nanoparticles. The effect of liquid crystals doped with inorganic semiconducting, and ferroelectric nanoparticles are summarised in Table 3.

6 Biomaterials in liquid crystal

Having discussed the formation of lyotropic liquid crystals from a range of inorganic materials, it should be pointed out that also other anisotropic materials exhibit very similar behaviour. Following Onsager's description, also anisotropic biological nanostructures can exhibit lyotropic liquid crystalline behaviour, with cellulose nanocrystals (CNC) (Dong et al., 1996), Deoxyribonucleic acid (DNA) (Strzelecka et al., 1988) and the rod-like structure of the Tobacco mosaic virus (TMV) (Bawden et al., 1936) being the most prominent examples.

6.1 Tobacco mosaic virus

TMV is a RNA virus that affects a variety of plants and especially tobacco plants. The infected leaves exhibit a mosaic-like pattern, hence the name. The TMV virus has a rod-like structure with a relatively high aspect ratio, generally approximately 200–300 nm in length and about 20 nm wide. In 1936, the TMV was first reported to exhibit liquid crystalline behaviour through X-ray experiments at a certain concentration (13–23 wt%) (Bawden et al., 1936). Oldenbourg et al. (1988) investigated TMV's orientational order, transitioning from the isotropic to the nematic phases via a biphasic region for increasing concentration. The liquid crystalline state of TMVs was experimentally investigated in detail by Fraden et al. (1993) and the phase diagram was established computationally by Graf and Löwen (1999) showing also a smectic phase and a colloidal crystal phase in addition to the nematic, as shown in Figure 15. Further, the cholesteric phase (Dogic and Fraden, 2000), the smectic phase (Dogic and Fraden, 1997) and the colloidal crystal phase (Graf and Löwen, 1999) have also been observed in other virus suspensions.

6.2 DNA

DNA is the macromolecule that carries the genetic information of organisms within a double helical structure. As a macromolecule, DNA can be seen as a nanoparticle with extremely large aspect ratio, in a sense similar to carbon nanotubes, nanowires or imogolite, which can all form lyotropic liquid crystals, only that DNA is a biomaterial. This was demonstrated in 1988, when Strzelecka et al. (1988) revealed various liquid crystal phases of DNA at high concentration, including cholesteric and smectic-like phases. Leforstier and Livolant (1994) reported that at high concentration DNA exhibits also a Blue phase.

TABLE 3 Effect of inorganic semiconducting/ferroelectric nanoparticles on the electric properties of liquid crystal.

Material	Liquid crystals	Results	Ref.
ZnO, TiO_2	NLC (MJ9915)	V_{th} ↓	Chen et al. (2009)
CdSe	NLC	V_{th} ↓	Williams et al. (2005)
ZnO	FLC (KCFLC 75)	V_{th} ↓	Joshi et al. (2010)
CdSe	CE8, CE6	BPs range ↑	Karatairi et al. (2010)
ZnO	MBBA	V_{th} ↑, dielectric anisotropy ↑, elastic constant ↑, viscosity ↑	Tripathi et al. (2013b)
$MnTiO_3$	6CHBT	T_{NI} ↑, dielectric anisotropy ↑, V_{th} ↓, elastic constant ↓	Elkhalgi et al. (2018b)
$Sn_2P_2S_6$	NLC (ZLI-4801)	Dielectric response ↑, order parameter ↑, dielectric anisotropy ↑, dielectric permittivity ↑, V_{th} ↓	Reznikov et al. (2003), Ouskova et al. (2003), Buchnev et al. (2003), Buchnev et al. (2004), Reznikov et al. (2005)
$Sn_2P_2S_6$	CLC (ZLI-4801 + R811)	Birefringence ↑, dielectric anisotropy ↑	Kurochkin et al. (2009)
$BaTiO_3$	MLC-6609	Order parameter ↑, T_{NI} ↑, birefringence ↑, dielectric anisotropy ↑, elastic constant ↑	Li et al. (2006a), Li et al. (2006b)
$BaTiO_3$	FLC (CS1024)	Polarisation ↑, response time ↓, dielectric constant ↓	Liang et al. (2010)
$BaTiO_3$	5CB	V_{th} ↑, elastic constant ↑ at $BaTiO_3$ > 1%	Al-Zangana et al. (2017b)
	TL205, 5CB	V_{th} ↓	Cook et al. (2010), Blach et al. (2010)
	5CB	V_{th} ↑ did not change significantly	Glushchenko et al. (2006), Klein et al. (2013)
	6CHBT	V_{th} ↑	Paul et al. (2011)
$Sn_2P_2S_6$, $BaTiO_3$	TL205, 18523	V_{th} ↓, elastic constant ↓, dielectric constant ↑	Podoliak et al. (2014)

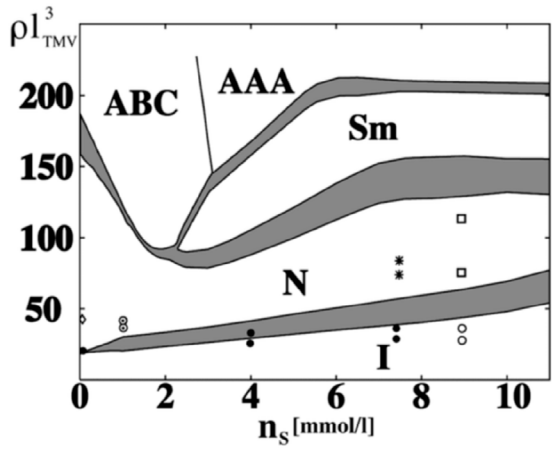

FIGURE 15
Phase diagram of the tobacco mosaic virus. The isotropic (I), nematic (N), and smectic-A phase (Sm) are observed, together with different colloidal crystal phases (Graf and Löwen, 1999).

6.3 Cellulose nanocrystals (CNCs)

CNCs are nanoscale particles obtained from cellulose fibres. These cellulose nanocrystals can be dispersed in different solvents, largely following Onsager's model. The rod-like CNCs particles with a relatively high aspect ratio (length 100 μm and width 10 μm) enable to form lyotropic LC in a suitable solvent (Rojas, 2016; George and Sabapathi, 2015). Due to the inherent chirality of the CNC particles dispersed in an aqueous solution exhibit a lyotropic cholesteric (chiral nematic) phase (Gray, 2016; Gray and Mu, 2015). In the lyotropic phase, aggregates of the CNCs form a helical superstructure and display a typical fingerprint texture, where the distance between the dark lines in the texture is equal to half of the helical pitch, as shown in Figure 16 (Dong et al., 1996) To observe the fingerprint pattern the helix axis is oriented in the plane of the substrate. On the contrary, if the helix axis is oriented perpendicular to the substrate plane, the phenomenon of selective reflection of circularly polarised light is observed, where a wavelength $\lambda_0 = \langle n \rangle P$ is reflected, with $\langle n \rangle$ the average refractive index and P the pitch of the helix. The reflected photonic bandgap $\Delta\lambda = \Delta nP$ is related to the birefringence Δn. In general, with an increasing concentration of CNCs, the pitch decreases, and the volume fraction of the anisotropic phase increases (Gray and Mu, 2015; Hirai et al., 2009). When the solvent in the CNCs suspension evaporates, the dried solid film can retain the chiral nematic order, and the pitch reduces to the visible range of the spectrum, indicating the rod-like nanoparticles self-assemble into a helical array (Revol et al., 1992).

The CNC nanoparticles dispersed in water exhibit the common phase behaviour as predicted by the Onsager description, starting from the isotropic phase at low CNC concentration, followed by a biphasic region, and finally transitioning into a lyotropic liquid crystalline cholesteric phase (Gray, 2016; Beck-Candanedo et al., 2005; Lagerwall et al., 2014). CNC nanoparticles are eco-friendly materials that show promising potential in thin film application, including variable narrow-range selective reflection (Fernandes et al., 2017; Saha and Davis, 2018), drug delivery (Schram et al.,

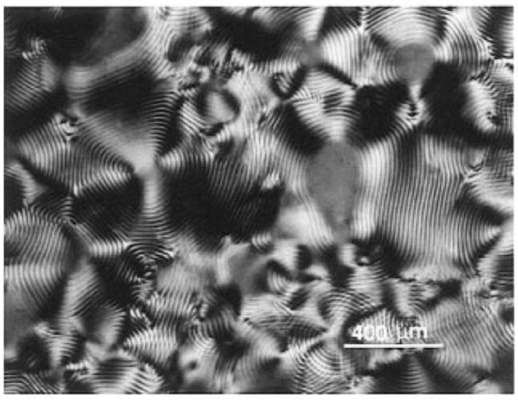

FIGURE 16
POM image of cellulose suspension exhibit cholesteric LC phase, showing fingerprint texture (Dong et al., 1996).

2015; Siepmann and Peppas, 2012) and sensors (Islam et al., 2018; Liu H. et al., 2019).

Biomaterials in liquid crystal research provide interesting opportunities for future applications (Zhang Z. et al., 2023), such as biosensor (Tan et al., 2010; Yang et al., 2012; Liao S. et al., 2012) and alignment reorientation (Price and Schwartz, 2008; Nakata et al., 2008), wearable devices (Zhang et al., 2022). Figure 17 shows the mechanism of a LC-based sensor. The nematic LC is aligned homeotropically at the solid substrate and planar at the water-LC interface, which leads to birefringence and the sensor appearing bright between crossed polarisers (Figure 17B). After introducing external stimulation, for example by adding surfactant molecules (L-α-dilauroyl phosphatidylcholine (L-DLPC)), the alignment of the LC molecules is changed, and a vesicle-like structure is formed at the water-LC interface containing the lipid molecules and water. The morphology difference extends into the LC layer and can easily be observed under POM with a decreased birefringence, because the formally planar oriented LC molecules now partially adopt a homeotropic orientation (Figure 17C). After 2 h of immersion, all LC molecules adopt a homeotropic orientation and the sensor appears black between crossed polarisers (Figure 17D).

7 Future scope, outlook and summary

The combination of nanomaterials and liquid crystals provides several key effects, such as enhanced electro-optical properties,

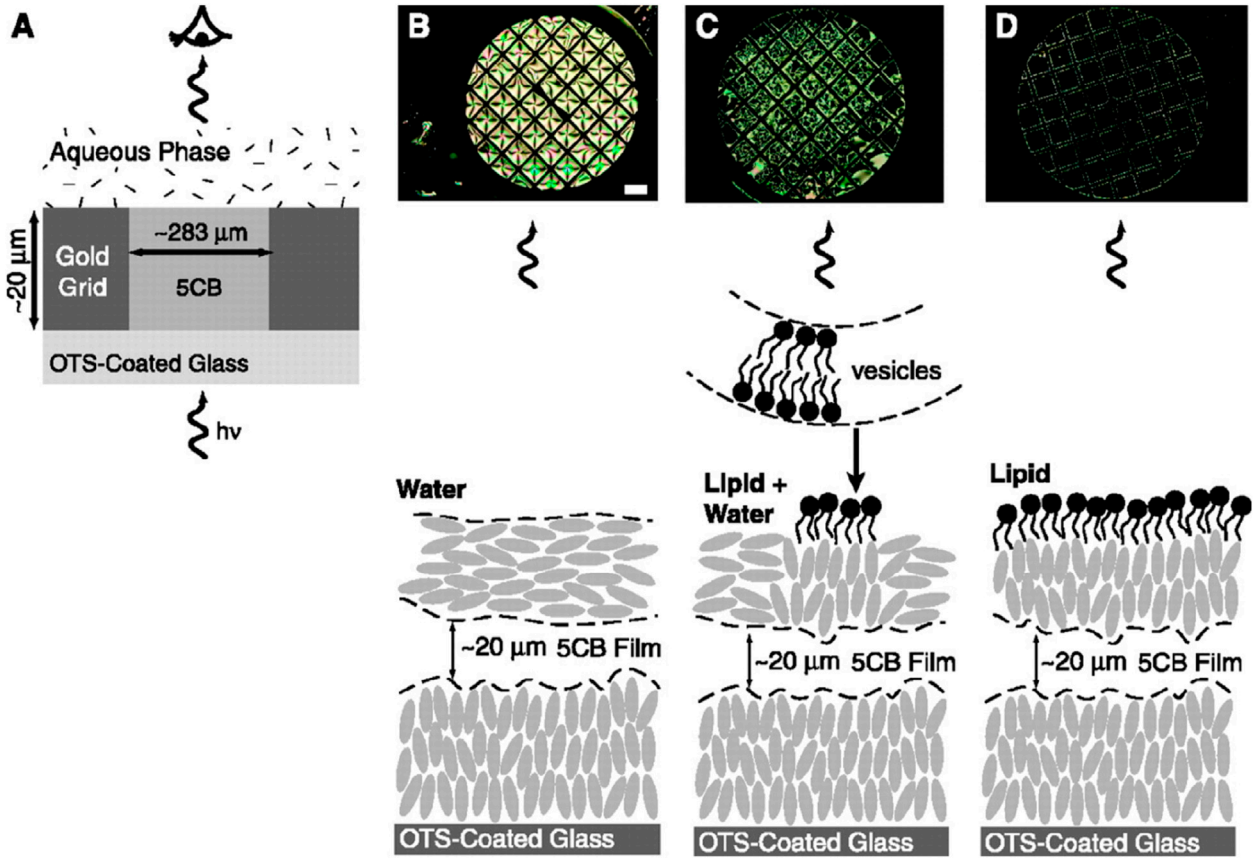

FIGURE 17
(A) Schematic illustration of a LC sensor. **(B–D)** Optical images and cartoon representations depicting the anchoring of nematic LC 5CB and the state of the water-5CB interface after injection of dispersion of vesicles formed form 0.1 mM L-DLPC in tris-buffered saline **(B)** corresponds to the immediate state, **(C, D)** represent the conditions at 10–20 min and 2 h, respectively. The optical images transition from a bright domain in **(B)** to a dark domain in **(C)** and finally appear uniformly dark in **(D)** (Brake et al., 2003).

phase transition tuning, improved alignment arrangement, self-organisation, dielectric properties and increased conductivity. There are potential applications for this combination beyond displays. Nanocrystals are used in the pharmaceutical industry as soluble drugs (Deori and Deka, 2013). Lyotropic liquid crystals can act as surfactant source in nanoparticles synthesis (Smaisim et al., 2023). The inkjet printing nanoparticle reorient the LC molecules is used in toxic gas sensor devices (Prévôt et al., 2020).

Working through the recent literature on nanoparticles dispersed in liquid crystals, one can identify three major current areas of research, (i) the tuning of physical properties of the composite materials, often for electro-optic applications, including photonics and plasmonics; (ii) the use of nanoparticle dispersed polymer dispersed liquid crystals (PDLC), polymer stabilised liquid crystals (PSLC) and liquid crystal elastomers (LCE), often related to Smart Glass and Privacy Windows, and; (iii) sensor applications based on nanoparticle-dispersed liquid crystals.

In the first category a whole range of physical parameters are tuned, starting with enhanced birefringence through ferric oxide nanoparticles from Δn = 0.185 to 0.2, also due to an increase in order nematic parameter (Tripathi et al., 2023). The dielectric anisotropy as well as conductivity was tuned by concentration varied addition of iron oxide (Kovalchuk et al., 2022). But also CuO enhanced the dielectric anisotropy and the relaxation frequency of ionic contamination (Jaiswal et al., 2023). Of importance for electro-optic switching processes are obviously the elastic constants and viscosities (Brouckaert et al., 2022). Thermal stability, dielectric anisotropy and related electro-optic parameters can be enhanced for example by the addition of silver nanoparticles (Verma et al., 2024), while layered perovskite nanoparticles have been used to tune the dielectric properties, but also memory effects (Varshney et al., 2023a).

The dispersion of carbon and graphene quantum dots enhances the contrast ratio, birefringence, and order parameter, while the dielectric anisotropy slightly decreases with addition of the dots and the conductivity increases (Neha et al., 2023a). The influence of carbon dots on a large variety of different physical parameters, such as elasticity, threshold voltage, dielectric behaviour and response times has been reviewed in detail in (Neha et al., 2023b). An interesting approach to tune properties has been suggested by the use of multifunctional nanoparticles, combining chiral, magnetic and photosensitive properties (Poryvai et al., 2022).

The second category of composite liquid crystalline systems involves those with nanoparticles and polymers, thus LC-polymer-nanoparticle multicomponent composites as they are used in PDLCs, PSCTs and LCEs. Most work done in this direction was on polymer dispersed liquid crystals, as these represent excellent candidates for smart windows. Nanoparticles of varying composition all seem to lead to similar effects on the electro-optic parameters, when doped into PDLCs. These include a reduction of threshold voltage, increased contrast, decreased switching times and an overall lower voltage performance, thus lower power consumption. This is observed for metal oxides (Malik and Singh, 2023) and in particular MgO (Zhao et al., 2022), TiO_2 (Wang X. et al., 2022), Al_2O_3 (Jia et al., 2022) and CeO_2 (Jinqian et al., 2022) to name some examples. Co-doped systems with fluorescent molecules together with nanoparticles were reported in (Lu et al., 2024). The progress in the field of multicomponent composites has recently been reviewed in (Gridyakina et al., 2023), while the thermos-electro-optics and dielectric behaviour showed promise for PDLC-based switchable windows (Katariya-Jain et al., 2024).

While most of the work so far has been reported for PDLCs, thus systems with a relatively high polymer content (~70%), a recent study of such a multicomponent composite at the low concentration range of polymer (~3%) has focussed on the properties of PSCTs (Gruzdenko and Dierking, 2023). For weakly cross-linked polymers, i.e., liquid crystal elastomers (LCEs) an enhanced mechanosensitivity has recently been reported for nanoparticle-dispersed systems (Sun et al., 2022). The properties and applications of LCEs doped with metallic and magnetic nanoparticles as well as carbon allotropes, has been reviewed in (Wang Y. et al., 2022).

The field of sensor applications on the basis of liquid crystals in general currently experiences a great interest within the soft matter community. A number of such sensors are based on photonic band gap materials, such as the cholesteric phase, which has long been used for temperature measurements. The performance of these temperature sensors can be improved through composite materials such as LC-Fe2O3 nanoparticle materials (Miao et al., 2022). The use of magnetic nanoparticles in doped photonic fibre sensors (Zhang R. et al., 2023) allows the detection of voltages, temperatures and magnetic fields. Yet many other sensors have been realised, stress and strain sensors, chirality sensors, morphology sensors, or gas sensors, as reviewed in (Leal-Junior et al., 2023).

Nevertheless, the main impact can be seen in the area of biosensors and healthcare sensors for example for DNA, bacterial infections, or cancer cells (Leal-Junior et al., 2023). Specific sensors for glucose (Kim et al., 2013), cholesterol (Tyagi et al., 2014), heavy metals (Du et al., 2021), or enzymes (Ping et al., 2021) have been developed on the basis of liquid crystal phases. Recently, an ultra-sensitive DNAzyme-based (DNA enzyme, catalytic DNA) sensor was developed with Au nanoparticles for signal amplification (Wang Z. et al., 2022). Similarly, also based on Au nanoparticle signal amplification, a biosensor for the detection of human chorionic gonadotropin (HCG antigen) has been suggested, which is of importance for early pregnancy testing (Wang et al., 2024). A review of the principles, realisation and applications of liquid crystal based biosensors has recently been provided by Wang et al. (Wang H. et al., 2022).

Currently, the three discussed areas above seem to be the main fields of research in the investigations of liquid crystal – nanoparticle hybrid materials. This is not to say that there are not any further fields of interest, for example photonics where the alignment of liquid crystals may be controlled via indium tin oxide (ITO) nanoparticles (Varshney et al., 2023b; Varshney et al., 2023c). The whole area of flexible photonic films on the basis of lyotropic cholesteric cellulose nanocrystals is still being evaluated also with respect to sensors (Saraiva et al., 2024) and the possibility of inkjet printing CNC lyotropics into photonic patterns does of course has its appeal (Williams et al., 2024). Also plasmonic devices, especially with gold or silver nanoparticles in liquid crystals (Yakovkin and Reshetnyak, 2023) will continue to find their interest in the future. The applicability of the discussed systems in nanotechnology is surely not fully exhausted by the possibilities of nanoparticle synthesis in liquid crystals and subsequent self-assembly (Smaisim et al., 2023), as can be seen in the collective ordering of magnetic nanoparticles (Dierking et al., 2017; Mertelj and Lisjak, 2017; Lacková et al., 2024).

In this review, we provided an overview of nanomaterials in thermotropic and lyotropic liquid crystals. We summarised the dispersion of various kinds of nanomaterials including metal nanoparticles, carbon allotropies, inorganic nanoparticles, ferroelectric and semiconducting nanoparticles with liquid crystals. The interaction between these nanoparticles and liquid crystals leads to changes in optical and electrical properties, thermal stability and alignment control, among other properties. The specific properties induced by the nanoparticles have been discussed in term of size, concentration and shape. Additionally, we introduced various anisotropic nanoparticles that can self-assemble into lyotropic liquid crystalline phases, such as nanorods, nanowires, nanotubes and nanoplates. Last but not least, some biological nanomaterials like TMV, DNA and CNC were introduced which can also form lyotropic liquid crystals. The integration of nanomaterial and liquid crystals is a growing and progressing research area, leading to the development of novel applications in various fields.

Author contributions

C-HC: Writing–original draft, Writing–review and editing. ID: Conceptualization, Project administration, Resources, Supervision, Validation, Visualization, Writing–original draft, Writing–review and editing.

Funding

The author(s) declare that no financial support was received for the research, authorship, and/or publication of this article.

Conflict of interest

The authors declare that the research was conducted in the absence of any commercial or financial relationships that could be construed as a potential conflict of interest.

Generative AI statement

The author(s) declare that no Generative AI was used in the creation of this manuscript.

Publisher's note

References

Aboutalebi, S. H., Gudarzi, M. M., Zheng, Q. B., and Kim, J. (2011). Spontaneous formation of liquid crystals in ultralarge graphene oxide dispersions. *Adv. Funct. Mater.* 21 (15), 2978–2988. doi:10.1002/adfm.201100448

Al-Zangana, S., Iliut, M., Boran, G., Turner, M., Vijayaraghavan, A., and Dierking, I. (2016b). Dielectric spectroscopy of isotropic liquids and liquid crystal phases with dispersed graphene oxide. *Sci. Rep.* 6 (1), 31885. doi:10.1038/srep31885

Al-Zangana, S., Iliut, M., Turner, M., Vijayaraghavan, A., and Dierking, I. (2016a). Properties of a thermotropic nematic liquid crystal doped with graphene oxide. *Adv. Opt. Mater.* 4 (10), 1541–1548. doi:10.1002/adom.201600351

Al-Zangana, S., Iliut, M., Turner, M., Vijayaraghavan, A., and Dierking, I. (2017a). Confinement effects on lyotropic nematic liquid crystal phases of graphene oxide dispersions. *2D Mater.* 4 (4), 041004. doi:10.1088/2053-1583/aa843a

Al-Zangana, S., Turner, M., and Dierking, I. (2017b). A comparison between size dependent paraelectric and ferroelectric BaTiO3 nanoparticle doped nematic and ferroelectric liquid crystals. *J. Appl. Phys.* 121 (8). doi:10.1063/1.4976859

Baik, I.-S., Jeon, S. Y., Lee, S. H., Park, K. A., Jeong, S. H., An, K. H., et al. (2005). Electrical-field effect on carbon nanotubes in a twisted nematic liquid crystal cell. *Appl. Phys. Lett.* 87, 87. doi:10.1063/1.2158509

Barmatov, E. B., Pebalk, D. A., and Barmatova, M. V. (2004). Influence of silver nanoparticles on the phase behavior of side-chain liquid crystalline polymers. *Langmuir* 20 (25), 10868–10871. doi:10.1021/la048601h

Basu, R. (2014). Effects of graphene on electro-optic switching and spontaneous polarization of a ferroelectric liquid crystal. *Appl. Phys. Lett.* 105, 105. doi:10.1063/1.4896112

Basu, R., and Iannacchione, G. S. (2010). Orientational coupling enhancement in a carbon nanotube dispersed liquid crystal. *Phys. Rev. E* 81 (5), 051705. doi:10.1103/physreve.81.051705

Basu, R., Kinnamon, D., and Garvey, A. (2015). Nano-electromechanical rotation of graphene and giant enhancement in dielectric anisotropy in a liquid crystal. *Appl. Phys. Lett.* 106, 106. doi:10.1063/1.4921752

Bawden, F., Pirie, N. W., Bernal, J. D., and Fankuchen, I. (1936). Liquid crystalline substances from virus-infected plants. *Nature* 138, 1051–1052. doi:10.1038/1381051a0

Beck-Candanedo, S., Roman, M., and Gray, D. G. (2005). Effect of reaction conditions on the properties and behavior of wood cellulose nanocrystal suspensions. *Biomacromolecules* 6 (2), 1048–1054. doi:10.1021/bm049300p

Behabtu, N., Lomeda, J. R., Green, M. J., Higginbotham, A. L., Sinitskii, A., Kosynkin, D. V., et al. (2010). Spontaneous high-concentration dispersions and liquid crystals of graphene. *Nat. Nanotechnol.* 5 (6), 406–411. doi:10.1038/nnano.2010.86

Bisoyi, H. K., and Kumar, S. (2011). Liquid-crystal nanoscience: an emerging avenue of soft self-assembly. *Chem. Soc. Rev.* 40 (1), 306–319. doi:10.1039/b901793n

Blach, J.-F., Saitzek, S., Legrand, C., Dupont, L., Henninot, J. F., and Warenghem, M. (2010). BaTiO3 ferroelectric nanoparticles dispersed in 5CB nematic liquid crystal: synthesis and electro-optical characterization. *J. Appl. Phys.* 107, 107. doi:10.1063/1.3369544

Blanc, C., Coursault, D., and Lacaze, E. (2013). Ordering nano-and microparticles assemblies with liquid crystals. *Liq. Cryst. Rev.* 1 (2), 83–109. doi:10.1080/21680396.2013.818515

Brake, J. M., Daschner, M. K., Luk, Y. Y., and Abbott, N. L. (2003). Biomolecular interactions at phospholipid-decorated surfaces of liquid crystals. *Science* 302 (5653), 2094–2097. doi:10.1126/science.1091749

Bravo-Sanchez, M., Simmons, T. J., and Vidal, M. (2010). Liquid crystal behavior of single wall carbon nanotubes. *Carbon* 48 (12), 3531–3542. doi:10.1016/j.carbon.2010.05.051

Brinchi, L., Cotana, F., Fortunati, E., and Kenny, J. (2013). Production of nanocrystalline cellulose from lignocellulosic biomass: technology and applications. *Carbohydr. Polym.* 94 (1), 154–169. doi:10.1016/j.carbpol.2013.01.033

Brochard, F., and De Gennes, P. (1970). Theory of magnetic suspensions in liquid crystals. *J. de Physique* 31 (7), 691–708. doi:10.1051/jphys:01970003107069100

Brouckaert, N., Podoliak, N., Orlova, T., Bankova, D., De Fazio, A. F., Kanaras, A. G., et al. (2022). Nanoparticle-induced property changes in nematic liquid crystals. *Nanomaterials* 12 (3), 341. doi:10.3390/nano12030341

Buchnev, O., Glushchenko, A. V., Reznikov, Y., Reshetnyak, V. Y., Tereshchenko, O., and West, J.L. (2003). Diluted ferroelectric suspension of Sn2P2S6 nanoparticles in nematic liquid crystal. *Ninth Int. Conf. Nonlinear Opt. Liq. Photorefractive Cryst.* 5257, 7–12. doi:10.1117/12.545780

Buchnev, O., Ouskova, E., Reznikov, Y., Reshetnyak, V., Kresse, H., and Grabar, A. (2004). Enhanced dielectric response of liquid crystal ferroelectric suspension. *Molecular Crystals and Liquid Crystals* 422(1), 47–55. doi:10.1080/15421400490502012

Bukowczan, A., Hebda, E., and Pielichowski, K. (2021). The influence of nanoparticles on phase formation and stability of liquid crystals and liquid crystalline polymers. *J. Mol. Liq.* 321, 114849. doi:10.1016/j.molliq.2020.114849

Cao, W., Muñoz, A., Palffy-Muhoray, P., and Taheri, B. (2002). Lasing in a three-dimensional photonic crystal of the liquid crystal blue phase II. *Nat. Mater.* 1 (2), 111–113. doi:10.1038/nmat727

Chaudhary, A., Malik, P., Mehra, R., and Raina, K. (2012). Electro-optic and dielectric studies of silica nanoparticle doped ferroelectric liquid crystal in SmC* phase. *Phase Transitions* 85 (3), 244–254. doi:10.1080/01411594.2011.624274

Chen, W.-T., Chen, P.-S., and Chao, C.-Y. (2009). Effect of doped insulating nanoparticles on the electro-optical characteristics of nematic liquid crystals. *Jpn. J. Appl. Phys. (2008).* 48 (1R), 015006. doi:10.1143/jjap.48.015006

Chigrinov, V. G. (1999). *Liquid crystal devices: physics and applications*.

Chigrinov, V. G., and Kwok, H.-S. (2013) *Photoalignment of liquid crystals: applications to fast response ferroelectric liquid crystals and rewritable photonic devices. Progress in Liquid Crystal Science and Technology: in Honor of Shunsuke Kobayashi's 80th Birthday*. 199–226.

Choudhary, A., Singh, G., and Biradar, A. M. (2014). Advances in gold nanoparticle–liquid crystal composites. *Nanoscale* 6 (14), 7743–7756. doi:10.1039/c4nr01325e

Chu, G., Wang, X., Chen, T., Gao, J., Gai, F., Wang, Y., et al. (2015). Optically tunable chiral plasmonic guest–host cellulose films weaved with long-range ordered silver nanowires. *ACS Appl. Mater. Interfaces* 7 (22), 11863–11870. doi:10.1021/acsami.5b01478

Chu, K., Chao, C. Y., Chen, Y. F., Wu, Y. C., and Chen, C. C. (2006). Electrically controlled surface plasmon resonance frequency of gold nanorods. *Appl. Phys. Lett.* 89, 89. doi:10.1063/1.2335812

Chuang, I., Durrer, R., Turok, N., and Yurke, B. (1991). Cosmology in the laboratory: defect dynamics in liquid crystals. *Science* 251 (4999), 1336–1342. doi:10.1126/science.251.4999.1336

Chuard, T., and Deschenaux, R. (1996). First fullerene[60]-containing thermotropic liquid crystal. *Prelim. Commun. Helvetica Chim. acta* 79 (3), 736–741. doi:10.1002/hlca.19960790316

Cîrtoaje, C., Petrescu, E., and Stoian, V. (2015). Electrical Freedericksz transitions in nematic liquid crystals containing ferroelectric nanoparticles. *Phys. E Low-dimensional Syst. Nanostructures* 67, 23–27. doi:10.1016/j.physe.2014.11.004

Clancy, A. J., Bayazit, M. K., Hodge, S. A., Skipper, N. T., Howard, C. A., and Shaffer, M. S. P. (2018). Charged carbon nanomaterials: redox chemistries of fullerenes, carbon nanotubes, and graphenes. *Chem. Rev.* 118 (16), 7363–7408. doi:10.1021/acs.chemrev.8b00128

Coles, H. J., and Pivnenko, M. N. (2005). Liquid crystal 'blue phases' with a wide temperature range. *Nature* 436 (7053), 997–1000. doi:10.1038/nature03932

Collings, P. J., and Hird, M. (2017). *Introduction to liquid crystals chemistry and physics*. London, United Kingdom: Taylor & Francis.

Collins, P. G., and Avouris, P. (2000). Nanotubes for electronics. *Sci. Am.* 283 (6), 62–69. doi:10.1038/scientificamerican1200-62

Cook, G., Barnes, J. L., Basun, S. A., Evans, D. R., Ziolo, R. F., Ponce, A., et al. (2010). Harvesting single ferroelectric domain stressed nanoparticles for optical and ferroic applications. *J. Appl. Phys.* 108, 108. doi:10.1063/1.3477163

Coondoo, I., Goel, P., Malik, A., and Biradar, A. M. (2011). Dielectric and polarization properties of BaTiO3 nanoparticle/ferroelectric liquid crystal colloidal suspension. *Integr. Ferroelectr.* 125 (1), 81–88. doi:10.1080/10584587.2011.574078

Crooks, R. M., Zhao, M., Sun, L., Chechik, V., and Yeung, L. K. (2001). Dendrimer-encapsulated metal nanoparticles: synthesis, characterization, and applications to catalysis. *Accounts Chem. Res.* 34 (3), 181–190. doi:10.1021/ar000110a

Dalir, N., Javadian, S., Kakemam, J., and Yousefi, A. (2018). Evolution of electro-chemical and electro-optical properties of nematic liquid crystal doped with graphene oxide. *J. Mol. Liq.* 265, 398–407. doi:10.1016/j.molliq.2018.05.138

Dan, B., Behabtu, N., Martinez, A., Evans, J. S., Kosynkin, D. V., Tour, J. M., et al. (2011). Liquid crystals of aqueous, giant graphene oxide flakes. *Soft Matter* 7 (23), 11154–11159. doi:10.1039/c1sm06418e

Daniel, M.-C., and Astruc, D. (2004). Gold Nanoparticles: assembly, supramolecular chemistry, quantum-size-related properties, and applications toward biology, catalysis, and nanotechnology. *Chem. Rev.* 104 (1), 293–346. doi:10.1021/cr030698+

Dellinger, T. M., and Braun, P. V. (2004). Lyotropic liquid crystals as nanoreactors for nanoparticle synthesis. *Chem. Mater.* 16 (11), 2201–2207. doi:10.1021/cm0349194

Deori, K., and Deka, S. (2013). Morphology oriented surfactant dependent CoO and reaction time dependent Co 3 O 4 nanocrystals from single synthesis method and their optical and magnetic properties. *CrystEngComm* 15 (42), 8465–8474. doi:10.1039/c3ce41502c

Dierking, I. (2018). Nanomaterials in liquid crystals. *Nanomater. Liq. Cryst.* 8, 453. doi:10.3390/nano8070453

Dierking, I. (2019). Royal society of chemistry. *Polymer-modified Liq. Cryst*. doi:10.1039/9781788013321

Dierking, I., Casson, K., and Hampson, R. (2008). Reorientation dynamics of liquid crystal–nanotube dispersions. *Jpn. J. Appl. Phys. (2008).* 47 (8R), 6390. doi:10.1143/jjap.47.6390

Dierking, I., Heberle, M., Osipov, M. A., and Giesselmann, F. (2017). Ordering of ferromagnetic nanoparticles in nematic liquid crystals. *Soft Matter* 13 (26), 4636–4643. doi:10.1039/c7sm01029j

Dierking, I., and Martins Figueiredo, A. (2020). Neto, Novel trends in lyotropic liquid crystals. *Crystals* 10 (7), 604. doi:10.3390/cryst10070604

Dierking, I., and San, S. E. (2005). Magnetically steered liquid crystal-nanotube switch. *Appl. Phys. Lett.* 87, 87. doi:10.1063/1.2140069

Dierking, I., Scalia, G., and Morales, P. (2005). Liquid crystal–carbon nanotube dispersions. *J. Appl. Phys.* 97, 97. doi:10.1063/1.1850606

Dierking, I., Scalia, G., Morales, P., and LeClere, D. (2004). Aligning and reorienting carbon nanotubes with nematic liquid crystals. *Adv. Mater.* 16 (11), 865–869. doi:10.1002/adma.200306196

Diesselhorst, H., and Freundlich, H. (1915). On the double refraction of vanadine pentoxydsol. *Phys. Z* 16, 419–425.

Dogic, Z., and Fraden, S. (1997). Smectic phase in a colloidal suspension of semiflexible virus particles. *Phys. Rev. Lett.* 78 (12), 2417–2420. doi:10.1103/physrevlett.78.2417

Dogic, Z., and Fraden, S. (2000). Cholesteric phase in virus suspensions. *Langmuir* 16 (20), 7820–7824. doi:10.1021/la000446t

Dolganov, V., Meletov, K., and Ossipyan, Y. A. (1993). Orientational ordering of fullerene C70 in a smectic liquid crystal. *Jetp Letters C/C Of Pis'ma V Zhurnal Eksperimental'noi Teoreticheskoi Fiziki* 58, 127.

Dolgov, L., Kovalchuk, O., Lebovka, N., Tomylko, S., and Yaroshchuk, O. (2010). Liquid crystal dispersions of carbon nanotubes: dielectric, electro-optical and structural peculiarities, in Carbon nanotubes. *IntechOpen*. doi:10.5772/39439

Dong, X. M., Kimura, T., Revol, J. F., and Gray, D. G. (1996). Effects of ionic strength on the isotropic– chiral nematic phase transition of suspensions of cellulose crystallites. *Langmuir* 12 (8), 2076–2082. doi:10.1021/la950133b

Draude, A. P., Kalavalapalli, T. Y., Iliut, M., McConnell, B., and Dierking, I. (2020). Stabilization of liquid crystal blue phases by carbon nanoparticles of varying dimensionality. *Nanoscale Adv.* 2 (6), 2404–2409. doi:10.1039/d0na00276c

Du, X., Liu, Y., Wang, F., Zhao, D., Gleeson, H. F., and Luo, D. (2021). A fluorescence sensor for Pb^{2+} detection based on liquid crystals and aggregation-induced emission luminogens. *ACS Appl. Mater. Interfaces* 13 (19), 22361–22367. doi:10.1021/acsami.1c02585

Elkhalgi, H. H., Khandka, S., Singh, U. B., Pandey, K. L., Dabrowski, R., and Dhar, R. (2018a). Dielectric and electro-optical properties of a nematic liquid crystalline material with gold nanoparticles. *Liq. Cryst.* 45 (12), 1795–1801. doi:10.1080/02678292.2018.1487089

Elkhalgi, H. H., Khandka, S., Yadav, N., Dhar, R., and Dabrowski, R. (2018b). Effects of manganese (II) titanium oxide nano particles on the physical properties of a room temperature nematic liquid crystal 4-(trans-4′-n-hexylcyclohexyl) isothiocyanatobenzene. *J. Mol. Liq.* 268, 223–228. doi:10.1016/j.molliq.2018.07.044

Engels, T., and von Rybinski, W. (1998). Liquid crystalline surfactant phases in chemical applications. *J. Mater. Chem.* 8 (6), 1313–1320. doi:10.1039/a706141b

Fernandes, S. N., Almeida, P. L., Monge, N., Aguirre, L. E., Reis, D., de Oliveira, C. L. P., et al. (2017). Mind the microgap in iridescent cellulose nanocrystal films. *Adv. Mater.* 29 (2), 1603560. doi:10.1002/adma.201603560

Fraden, S., Maret, G., and Caspar, D. (1993). Angular correlations and the isotropic-nematic phase transition in suspensions of tobacco mosaic virus. *Phys. Rev. E* 48 (4), 2816–2837. doi:10.1103/physreve.48.2816

Garbovskiy, Y. A., and Glushchenko, A. V. (2010). Liquid crystalline colloids of nanoparticles: preparation, properties, and applications. *Solid State Phys.* 62, 1–74. doi:10.1016/B978-0-12-374293-3.00001-8

George, J., and Sabapathi, S. (2015). Cellulose nanocrystals: synthesis, functional properties, and applications. *Nanotechnol. Sci. Appl.* 8, 45–54. doi:10.2147/NSA.S64386

Gittins, D. I., Bethell, D., Schiffrin, D. J., and Nichols, R. J. (2000). A nanometre-scale electronic switch consisting of a metal cluster and redox-addressable groups. *Nature.* 408(6808), 67–69. doi:10.1038/35040518

Glushchenko, A., Cheon, C. I., West, J., Li, F., Büyüktanir, E., Reznikov, Y., et al. (2006). Ferroelectric particles in liquid crystals: recent frontiers. *Molecular Crystals and Liquid Crystals* 453(1), 227–237. doi:10.1080/15421400600653852

Gökçen, M., Yıldırım, M., and Köysal, O. (2012). Dielectric and AC electrical conductivity characteristics of liquid crystal doped with graphene. *Eur. Phys. Journal-Applied Phys.* 60 (3), 30104. doi:10.1051/epjap/2012120245

Gonçalves, D. P., Prévôt, M. E., Üstünel, Ş., Ogolla, T., Nemati, A., Shadpour, S., et al. (2021). Recent progress at the interface between nanomaterial chirality and liquid crystals. *Liq. Cryst. Rev.* 9 (1), 1–34. doi:10.1080/21680396.2021.1930596

Goodby, J. W. (2011). The nanoscale engineering of nematic liquid crystals for displays. *Liq. Cryst.* 38 (11-12), 1363–1387. doi:10.1080/02678292.2011.614700

Goodby, J. W., Saez, I., Cowling, S., Görtz, V., Draper, M., Hall, A., et al. (2008). Transmission and amplification of information and properties in nanostructured liquid crystals. *Angew. Chem. Int. Ed.* 47 (15), 2754–2787. doi:10.1002/anie.200701111

Graf, H., and Löwen, H. (1999). Phase diagram of tobacco mosaic virus solutions. *Phys. Rev. E* 59 (2), 1932–1942. doi:10.1103/physreve.59.1932

Gray, D. G. (2016). Recent advances in chiral nematic structure and iridescent color of cellulose nanocrystal films. *Nanomaterials* 6 (11), 213. doi:10.3390/nano6110213

Gray, D. G., and Mu, X. (2015). Chiral nematic structure of cellulose nanocrystal suspensions and films; polarized light and atomic force microscopy. *Materials* 8 (11), 7873–7888. doi:10.3390/ma8115427

Gridyakina, A., Kasian, N., Chychłowski, M. S., Kajkowska, M., and Lesiak, P. (2023). Advances in multicomponent systems: liquid crystal/nanoparticles/polymer. *Mater. Today Phys.* 38, 101258. doi:10.1016/j.mtphys.2023.101258

Gruzdenko, A., and Dierking, I. (2023). Electro-optic properties of polystyrene particle-laden polymer-stabilized liquid crystals. *J. Mater. Chem. C Mater.* 11 (16), 5438–5449. doi:10.1039/d3tc00437f

Grzelczak, M., Vermant, J., Furst, E. M., and Liz-Marzán, L. M. (2010). Directed self-assembly of nanoparticles. *ACS nano* 4 (7), 3591–3605. doi:10.1021/nn100869j

Gupta, M., Satpathy, I., Roy, A., and Pratibha, R. (2010). Nanoparticle induced director distortion and disorder in liquid crystal-nanoparticle dispersions. *J. Colloid Interface Sci.* 352 (2), 292–298. doi:10.1016/j.jcis.2010.08.027

Haynes, C. L., McFarland, A. D., Zhao, L., Van Duyne, R. P., Schatz, G. C., Gunnarsson, L., et al. (2003). Nanoparticle Optics: the importance of radiative dipole coupling in two-dimensional nanoparticle arrays. *J. Phys. Chem. B* 107 (30), 7337–7342. doi:10.1021/jp034234r

Hegmann, T., Qi, H., and Marx, V. M. (2007). Nanoparticles in liquid crystals: synthesis, self-assembly, defect formation and potential applications. *J. Inorg. Organomet. Polym. Mater.* 17, 483–508. doi:10.1007/s10904-007-9140-5

Herrington, M., Buchnev, O., Kaczmarek, M., and Nandhakumar, I. (2010). The effect of the size of BaTiO3 nanoparticles on the electro-optic properties of nematic liquid crystals. *Mol. Cryst. Liq. Cryst.* 527 (1), 72. doi:10.1080/15421406.2010.486362

Hinojosa, A., and Sharma, S. C. (2010). Effects of gold nanoparticles on electro-optical properties of a polymer-dispersed liquid crystal. *Appl. Phys. Lett.* 97, 97. doi:10.1063/1.3482942

Hirai, A., Inui, O., Horii, F., and Tsuji, M. (2009). Phase separation behavior in aqueous suspensions of bacterial cellulose nanocrystals prepared by sulfuric acid treatment. *Langmuir* 25 (1), 497–502. doi:10.1021/la802947m

Holt, L. A., Bushby, R. J., Evans, S. D., Burgess, A., and Seeley, G. (2008). A 106-fold enhancement in the conductivity of a discotic liquid crystal doped with only 1%w/w gold nanoparticles. *Journal of Applied Physics* 103 (6).

Hsu, C.-J., Huang, M. K., Tsai, P. C., Hsieh, C. T., Kuo, K. L., You, C. F., et al. (2018). The effects of silica nanoparticles on blue-phase liquid crystals. *Liq. Cryst.* 45 (2), 303–309. doi:10.1080/02678292.2017.1324645

Hu, J., Odom, T. W., and Lieber, C. M. (1999). Chemistry and physics in one dimension: synthesis and properties of nanowires and nanotubes. *Accounts Chem. Res.* 32 (5), 435–445. doi:10.1021/ar9700365

Hu, J., Yang, W., Manna, L., Wang, L. w., and Alivisatos, A. P. (2001). Linearly polarized emission from colloidal semiconductor quantum rods. *Science* 292 (5524), 2060–2063. doi:10.1126/science.1060810

Hummers, W. S., Jr, and Offeman, R. E. (1958). Preparation of graphitic oxide. *J. Am. Chem. Soc.* 80 (6), 1339. doi:10.1021/ja01539a017

Ibragimov, T. D., and Rzayev, R. M. (2020). Dielectric relaxation, electric conductivity, and electro-optic properties of SWCNT-doped liquid crystal 5CB. *Nanotub. Carbon Nanostructures* 28 (12), 982–988. doi:10.1080/1536383x.2020.1788543

Iijima, S. (1991). Helical microtubules of graphitic carbon. *nature* 354 (6348), 56–58. doi:10.1038/354056a0

Islam, M., Chen, L., Sisler, J., and Tam, K. C. (2018). Cellulose nanocrystal (CNC)–inorganic hybrid systems: synthesis, properties and applications. *J. Mater. Chem. B* 6 (6), 864–883. doi:10.1039/c7tb03016a

Jaiswal, M., Srivastava, G., Mishra, S., Kumar Singh, P., Dhar, R., and Dabrowski, R. (2023). Synthesis and characterization of semiconducting copper oxide nanoparticles and their impact on the physical properties of a nematic liquid crystalline material 4-pentyl-4′-cyanobiphenyl. *J. Mol. Liq.* 383, 122032. doi:10.1016/j.molliq.2023.122032

Jakli, A. (2010). Electro-mechanical effects in liquid crystals. *Liq. Cryst.* 37 (6-7), 825–837. doi:10.1080/02678291003784081

Jalili, R., Aboutalebi, S. H., Esrafilzadeh, D., Konstantinov, K., Moulton, S. E., Razal, J. M., et al. (2013). Organic solvent-based graphene oxide liquid crystals: a facile route toward the next generation of self-assembled layer-by-layer multifunctional 3D architectures. *Acs Nano* 7 (5), 3981–3990. doi:10.1021/nn305906z

Javadian, S., Dalir, N., and Kakemam, J. (2017). Non-covalent intermolecular interactions of colloidal nematic liquid crystals doped with graphene oxide. *Liq. Cryst.* 44 (9), 1341–1355. doi:10.1080/02678292.2016.1278051

Jayoti, D., Malik, P., and Singh, A. (2017). Analysis of morphological behaviour and electro-optical properties of silica nanoparticles doped polymer dispersed liquid crystal composites. *J. Mol. Liq.* 225, 456–461. doi:10.1016/j.molliq.2016.11.100

Jia, M., Zhao, Y., Gao, H., Wang, D., Miao, Z., Cao, H., et al. (2022). The Electro-optical study of Al2O3 nanoparticles doped polymer dispersed liquid crystal films. *Liq. Cryst.* 49 (1), 39–49. doi:10.1080/02678292.2021.1943024

Jiang, W., Yu, B., Liu, W., and Hao, J. (2007). Carbon nanotubes incorporated within lyotropic hexagonal liquid crystal formed in room-temperature ionic liquids. *Langmuir* 23 (16), 8549–8553. doi:10.1021/la700921w

Jinqian, L., Zhao, Y., Gao, H., Wang, D., Miao, Z., Cao, H., et al. (2022). Polymer dispersed liquid crystals doped with CeO2 nanoparticles for the smart window. *Liq. Cryst.* 49 (1), 29–38. doi:10.1080/02678292.2021.1942573

Joshi, T., Kumar, A., Prakash, J., and Biradar, A. M. (2010). Low power operation of ferroelectric liquid crystal system dispersed with zinc oxide nanoparticles. *Appl. Phys. Lett.* 96, 96. doi:10.1063/1.3455325

Karatairi, E., Rožič, B., Kutnjak, Z., Tzitzios, V., Nounesis, G., Cordoyiannis, G., et al. (2010). Nanoparticle-induced widening of the temperature range of liquid-crystalline blue phases. *Phys. Rev. E* 81 (4), 041703. doi:10.1103/physreve.81.041703

Katariya-Jain, A., Mhatre, M., Dierking, I., and Deshmukh, R. (2024). Enhanced thermo-electro-optical and dielectric properties of carbon nanoparticle-doped polymer dispersed liquid crystal based switchable windows. *J. Mol. Liq.* 393, 123575. doi:10.1016/j.molliq.2023.123575

Kaur, S., Singh, S. P., Biradar, A. M., Choudhary, A., and Sreenivas, K. (2007). Enhanced electro-optical properties in gold nanoparticles doped ferroelectric liquid crystals. *Appl. Phys. Lett.* 91, 91. doi:10.1063/1.2756136

Khatua, S., Manna, P., Chang, W. S., Tcherniak, A., Friedlander, E., Zubarev, E. R., et al. (2010). Plasmonic Nanoparticles–Liquid crystal composites. *J. Phys. Chem. C* 114 (16), 7251–7257. doi:10.1021/jp907923v

Kikuchi, H., Yokota, M., Hisakado, Y., Yang, H., and Kajiyama, T. (2002). Polymer-stabilized liquid crystal blue phases. *Nat. Mater.* 1 (1), 64–68. doi:10.1038/nmat712

Kim, J., Khan, M., and Park, S.-Y. (2013). Glucose sensor using liquid-crystal droplets made by microfluidics. *ACS Appl. Mater. Interfaces* 5 (24), 13135–13139. doi:10.1021/am404174n

Kim, J. E., Han, T. H., Lee, S. H., Ahn, C. W., Yun, J. M., and Kim, S. O. (2011b). Graphene oxide liquid crystals. *Angew. Chem. Int. Ed.* 50 (13), 3043–3047. doi:10.1002/anie.201004692

Kim, Y. H., Yoon, D. K., Jeong, H. S., Lavrentovich, O. D., and Jung, H. (2011a). Smectic liquid crystal defects for self-assembling of building blocks and their lithographic applications. *Adv. Funct. Mater.* 21 (4), 610–627. doi:10.1002/adfm.201001303

Klein, S., Richardson, R. M., Greasty, R., Jenkins, R., Stone, J., Thomas, M. R., et al. (2013). The influence of suspended nanoparticles on the Frederiks threshold of the nematic host. *Philosophical Transactions of the Royal Society A: Mathematical, Physical and Engineering Sciences* 371 (1988), 20120253. doi:10.1098/rsta.2012.0253

Kovalchuk, O., Kovalchuk, T., Tomašovičová, N., Timko, M., Zakutanska, K., Miakota, D., et al. (2022). Dielectric and electrical properties of nematic liquid crystals 6CB doped with iron oxide nanoparticles. *Comb. Eff. nanodopant concentration cell Thick.* 366, 120305. doi:10.1016/j.molliq.2022.120305

Krishna Prasad, S., Sandhya, K. L., Nair, G. G., Hiremath, U. S., Yelamaggad, C. V., and Sampath, S. (2006). Electrical conductivity and dielectric constant measurements of liquid crystal–gold nanoparticle composites. *Liq. Cryst.* 33 (10), 1121–1125. doi:10.1080/02678290600930980

Kroto, H. W., Heath, J. R., O'Brien, S. C., Curl, R. F., and Smalley, R. E. (1985). C60: buckminsterfullerene. *Nature* 318(6042), 162–163. doi:10.1038/318162a0

Kularatne, R. S., Kim, H., Boothby, J. M., and Ware, T. H. (2017). Liquid crystal elastomer actuators: synthesis, alignment, and applications. *J. Polym. Sci. Part B Polym. Phys.* 55 (5), 395–411. doi:10.1002/polb.24287

Kumar, A., Prakash, J., Mehta, D. S., Biradar, A. M., and Haase, W. (2009). Enhanced photoluminescence in gold nanoparticles doped ferroelectric liquid crystals. *Appl. Phys. Lett.* 95, 95. doi:10.1063/1.3179577

Kumar, A., Singh, D. P., and Singh, G. (2021). Recent progress and future perspectives on carbon-nanomaterial-dispersed liquid crystal composites. *J. Phys. D Appl. Phys.* 55 (8), 083002. doi:10.1088/1361-6463/ac2ced

Kumar, P., and Raina, K. (2012). Changes in the electro-optical behaviour of ferroelectric liquid crystal mixture via silica nanoparticles doping. *Opt. Mater.* 34 (11), 1878–1884. doi:10.1016/j.optmat.2012.05.022

Kumar, S. (2006). Self-organization of disc-like molecules: chemical aspects. *Chem. Soc. Rev.* 35 (1), 83–109. doi:10.1039/b506619k

Kumar, S., and Brock, J. (2001). *Liquid crystals: experimental study of physical properties and phase transitions*. Cambridge University Press.

Kurochkin, O., Buchnev, O., Iljin, A., Park, S. K., Kwon, S. B., Grabar, O., et al. (2009). A colloid of ferroelectric nanoparticles in a cholesteric liquid crystal. *J. Opt. A Pure Appl. Opt.* 11 (2), 024003. doi:10.1088/1464-4258/11/2/024003

Kurochkin, O., Atkuri, H., Buchnev, O., Glushchenko, A., Grabar, O., Karapinar, R., et al. (2010). Nano-colloids of Sn2P2S6 in nematic liquid crystal pentyl-cianobiphenile. *Condensed Matter Physics.* 13 (3), 33701.

Lacková, V., Schroer, M. A., Hähsler, M., Zakutanská, K., Behrens, S., Kopčanský, P., et al. (2024). The collective ordering of magnetic nanoparticles in a nematic liquid crystal. *J. Magn. Magn. Mater.* 589, 171616. doi:10.1016/j.jmmm.2023.171616

Lagerwall, J. P., Schütz, C., Salajkova, M., Noh, J., Park, J. H., Scalia, G., et al. (2014). Cellulose nanocrystal-based materials: from liquid crystal self-assembly and glass formation to multifunctional thin films. *NPG Asia Mater.* 6 (1), E80–E80. doi:10.1038/am.2013.69

Lagerwall, J. P., and Scalia, G. (2012). A new era for liquid crystal research: applications of liquid crystals in soft matter nano-bio- and microtechnology. *Curr. Appl. Phys.* 12 (6), 1387–1412. doi:10.1016/j.cap.2012.03.019

Landman, J., Paineau, E., Davidson, P., Bihannic, I., Michot, L. J., Philippe, A. M., et al. (2014). Effects of added silica nanoparticles on the nematic liquid crystal phase formation in beidellite suspensions. *J. Phys. Chem. B* 118 (18), 4913–4919. doi:10.1021/jp500036v

Lapanik, A., Rudzki, A., Kinkead, B., Qi, H., Hegmann, T., and Haase, W. (2012). Electrooptical and dielectric properties of alkylthiol-capped gold nanoparticle–ferroelectric liquid crystal nanocomposites: influence of chain length and tethered liquid crystal functional groups. *Soft Matter* 8 (33), 8722–8728. doi:10.1039/c2sm25991e

Lapointe, C. P., Mason, T. G., and Smalyukh, I. I. (2009). Shape-controlled colloidal interactions in nematic liquid crystals. *Science* 326 (5956), 1083–1086. doi:10.1126/science.1176587

Leal-Junior, A., Soares, M. S., de Almeida, P. M., and Marques, C. (2023). Cholesteric liquid crystals sensors based on nanocellulose derivatives for improvement of quality of human life: a review. *Adv. Sens. Res.* 2 (10), 2300022. doi:10.1002/adsr.202300022

Lee, C., Wei, X., Kysar, J. W., and Hone, J. (2008). Measurement of the elastic properties and intrinsic strength of monolayer graphene. *science* 321 (5887), 385–388. doi:10.1126/science.1157996

Lee, S.H., Lee, S.L., and Kim, H. (1998). Electro-optic characteristics and switching principle of a nematic liquid crystal cell controlled by fringe-field switching. *Appl. Phys. Lett.* 73 (20), 2881–2883. doi:10.1063/1.122617

Lee, W., and Chiu, C.-S. (2001). Observation of self-diffraction by gratings in nematic liquid crystals doped with carbon nanotubes. *Opt. Lett.* 26 (8), 521–523. doi:10.1364/ol.26.000521

Lee, W., Wang, C.-Y., and Shih, Y.-C. (2004). Effects of carbon nanosolids on the electro-optical properties of a twisted nematic liquid-crystal host. *Appl. Phys. Lett.* 85 (4), 513–515. doi:10.1063/1.1771799

Lee, W., Yeh, S. L., Chang, C. C., and Lee, C. C. (2001). Beam coupling in nanotube-doped liquid-crystal films. *Opt. Express* 9 (13), 791–795. doi:10.1364/oe.9.000791

Leforstier, A., and Livolant, F. (1994). DNA liquid crystalline blue phases. Electron microscopy evidence and biological implications. *Electron Microsc. Evid. Biol. Implic. Liq. Cryst.* 17 (5), 651–658. doi:10.1080/02678299408037336

Lehmann, W., Skupin, H., Tolksdorf, C., Gebhard, E., Zentel, R., Krüger, P., et al. (2001). Giant lateral electrostriction in ferroelectric liquid-crystalline elastomers. *Nature* 410 (6827), 447–450. doi:10.1038/35068522

Li, C.-Z., Yip, H.-L., and Jen, A.K.-Y. (2012). Functional fullerenes for organic photovoltaics. *J. Mater. Chem.* 22 (10), 4161–4177. doi:10.1039/c2jm15126j

Li, F., Buchnev, O., Cheon, C. I., Glushchenko, A., Reshetnyak, V., Reznikov, Y., et al. (2006a). Orientational coupling amplification in ferroelectric nematic colloids. *Phys. Rev. Lett.* 97 (14), 147801. doi:10.1103/physrevlett.97.147801

Li, F., West, J., Glushchenko, A., Cheon, C. I., and Reznikov, Y. (2006b). Ferroelectric nanoparticle/liquid-crystal colloids for display applications. *J. Soc. Inf. Disp.* 14 (6), 523–527. doi:10.1889/1.2210802

Li, L. S., and Alivisatos, A. P. (2003). Semiconductor nanorod liquid crystals and their assembly on a substrate. *Adv. Mater.* 15 (5), 408–411. doi:10.1002/adma.200390093

Li, L.-s., Hu, J., Yang, W., and Alivisatos, A. P. (2001). Band gap variation of size-and shape-controlled colloidal CdSe quantum rods. *Nano Lett.* 1 (7), 349–351. doi:10.1021/nl015559r

Li, L.-s., Walda, J., Manna, L., and Alivisatos, A. P. (2002). Semiconductor nanorod liquid crystals. *Nano Lett.* 2 (6), 557–560. doi:10.1021/nl0255146

Li, P., Wong, M., Zhang, X., Yao, H., Ishige, R., Takahara, A., et al. (2014). Tunable lyotropic photonic liquid crystal based on graphene oxide. *ACS photonics* 1 (1), 79–86. doi:10.1021/ph400093c

Li, X., Yang, C., Wang, Q., Jia, D., Hu, L., Peng, Z., et al. (2013). Enhanced birefringence for metallic nanoparticle doped liquid crystals. *Opt. Commun.* 286, 224–227. doi:10.1016/j.optcom.2012.09.001

Liang, H.-H., Xiao, Y. Z., Hsh, F. J., Wu, C. C., and Lee, J. Y. (2010). Enhancing the electro-optical properties of ferroelectric liquid crystals by doping ferroelectric nanoparticles. *Liq. Cryst.* 37 (3), 255–261. doi:10.1080/02678290903564403

Liao, S., Qiao, Y., Han, W., Xie, Z., Wu, Z., Shen, G., et al. (2012b). Acetylcholinesterase liquid crystal biosensor based on modulated growth of gold nanoparticles for amplified detection of acetylcholine and inhibitor. *Anal. Chem.* 84 (1), 45–49. doi:10.1021/ac202895j

Liao, S.-W., Hsieh, C. T., Kuo, C. C., and Huang, C. Y. (2012a). Voltage-assisted ion reduction in liquid crystal-silica nanoparticle dispersions. *Appl. Phys. Lett.* 101, 101. doi:10.1063/1.4760277

Lieber, C. M. (1998). One-dimensional nanostructures: chemistry, physics and applications. *Solid State Commun.* 107 (11), 607–616. doi:10.1016/s0038-1098(98)00209-9

Lisetski, L., Soskin, M., and Lebovka, N. (2014) "Carbon nanotubes in liquid crystals: fundamental properties and applications," in *Physics of liquid matter: modern problems: proceedings, kyiv, Ukraine, 23-27*. Springer, 2015.

Liu, H., Li, Q., Bu, Y., Zhang, N., Wang, C., Pan, C., et al. (2019b). Stretchable conductive nonwoven fabrics with self-cleaning capability for tunable wearable strain sensor. *Nano Energy* 66, 104143. doi:10.1016/j.nanoen.2019.104143

Liu, Q., Campbell, M. G., Evans, J. S., and Smalyukh, I. I. (2014b). Orientationally ordered colloidal co-dispersions of gold nanorods and cellulose nanocrystals. *Adv. Mater.* 26 (42), 7178–7184. doi:10.1002/adma.201402699

Liu, Q., Cui, Y., Gardner, D., Li, X., He, S., and Smalyukh, I. I. (2010). Self-alignment of plasmonic gold nanorods in reconfigurable anisotropic fluids for tunable bulk metamaterial applications. *Nano Lett.* 10 (4), 1347–1353. doi:10.1021/nl9042104

Liu, Q., Yuan, Y., and Smalyukh, I. I. (2014a). Electrically and optically tunable plasmonic guest–host liquid crystals with long-range ordered nanoparticles. *Nano Lett.* 14 (7), 4071–4077. doi:10.1021/nl501581y

Liu, X., Qi, G., Park, A. M. G., Rodriguez-Gonzalez, A., Enotiadis, A., Pan, W., et al. (2019a). Scalable synthesis of switchable assemblies of gold nanorod lyotropic liquid crystal nanocomposites. *Small* 15 (22), 1901666. doi:10.1002/smll.201901666

Lopatina, L. M., and Selinger, J. V. (2009). Theory of ferroelectric nanoparticles in nematic liquid crystals. *Phys. Rev. Lett.* 102 (19), 197802. doi:10.1103/physrevlett.102.197802

Lopatina, L. M., and Selinger, J. V. (2011). Maier-Saupe-type theory of ferroelectric nanoparticles in nematic liquid crystals. *Phys. Rev. E* 84 (4), 041703. doi:10.1103/physreve.84.041703

Lu, L., and Chen, W. (2010). Large-scale aligned carbon nanotubes from their purified, highly concentrated suspension. *ACS nano* 4 (2), 1042–1048. doi:10.1021/nn901326m

Lu, Y., Yang, D., Gao, H., Du, X., Zhao, Y., Wang, D., et al. (2024). Enhanced electro-optical properties of polymer-dispersed liquid crystals co-doped with fluorescent molecules and nanoparticles for multifunctional applications. *Chem. Eng. J.* 485, 149654. doi:10.1016/j.cej.2024.149654

Lynch, M. D., and Patrick, D. L. (2002). Organizing carbon nanotubes with liquid crystals. *Nano Lett.* 2 (11), 1197–1201. doi:10.1021/nl025694j

Malik, P., and Singh, A. K. (2023). Metal oxide alumina nanowire-induced polymer-dispersed liquid crystal composites for low power consumption smart windows. *J. Mol. Liq.* 378, 121573. doi:10.1016/j.molliq.2023.121573

Manepalli, R., Giridhar, G., Pardhasaradhi, P., Jayaprada, P., Tejaswi, M., Sivaram, K., et al. (2018). *Influence of ZnO nanoparticles dispersion in Liquid Crystalline compounds–Experimental studies*. *Mater. Today Proc.* 5 (1), 2666–2676. doi:10.1016/j.matpr.2018.01.047

Manohar, R., Yadav, S. P., Srivastava, A. K., Misra, A. K., Pandey, K. K., Sharma, P. K., et al. (2009). Zinc oxide (1% Cu) nanoparticle in nematic liquid crystal: dielectric and electro-optical study. *Jpn. J. Appl. Phys. (2008).* 48 (10R), 101501. doi:10.1143/jjap.48.101501

Mertelj, A., and Lisjak, D. (2017). Ferromagnetic nematic liquid crystals. *Liq. Cryst. Rev.* 5 (1), 1–33. doi:10.1080/21680396.2017.1304835

Mertelj, A., Lisjak, D., Drofenik, M., and Čopič, M. (2013). Ferromagnetism in suspensions of magnetic platelets in liquid crystal. *Nature* 504 (7479), 237–241. doi:10.1038/nature12863

Mertelj, A., Osterman, N., Lisjak, D., and Čopič, M. (2014). Magneto-optic and converse magnetoelectric effects in a ferromagnetic liquid crystal. *Soft Matter* 10 (45), 9065–9072. doi:10.1039/c4sm01625d

Miao, Y., Li, W., Wu, K., Sun, J., Cai, M., Zhao, T., et al. (2022). Performance improvement of capacitive liquid crystal temperature sensor by doping γ-Fe_2O_3 nanoparticles. *Molecular Crystals and Liquid Crystals* 740(1), 17–27. doi:10.1080/15421406.2022.2033063

Milette, J., Cowling, S. J., Toader, V., Lavigne, C., Saez, I. M., Bruce Lennox, R., et al. (2012). Reversible long range network formation in gold nanoparticle-nematic liquid crystal composites. *Soft Matter* 8 (1), 173–179. doi:10.1039/c1sm06604h

Mitov, M., Portet, C., Bourgerette, C., Snoeck, E., and Verelst, M. (2002). Long-range structuring of nanoparticles by mimicry of a cholesteric liquid crystal. *Nat. Mater.* 1 (4), 229–231. doi:10.1038/nmat772

Miyama, T., Thisayukta, J., Shiraki, H., Sakai, Y., Shiraishi, Y., Toshima, N., et al. (2004). Fast switching of frequency modulation twisted nematic liquid crystal display fabricated by doping nanoparticles and its mechanism. *Jpn. J. Appl. Phys. (2008).* 43 (5R), 2580. doi:10.1143/jjap.43.2580

Moreira, M., Carvalho, I. C. S., Cao, W., Bailey, C., Taheri, B., and Palffy-Muhoray, P. (2004). Cholesteric liquid-crystal laser as an optic fiber-based temperature sensor. *Appl. Phys. Lett.* 85 (14), 2691–2693. doi:10.1063/1.1781363

Morozov, S., Novoselov, K. S., Katsnelson, M. I., Schedin, F., Elias, D. C., Jaszczak, J. A., et al. (2008). Giant intrinsic carrier mobilities in graphene and its bilayer. *Phys. Rev. Lett.* 100 (1), 016602. doi:10.1103/physrevlett.100.016602

Mrukiewicz, M., Kowiorski, K., Perkowski, P., Mazur, R., and Djas, M. (2019). Threshold voltage decrease in a thermotropic nematic liquid crystal doped with graphene oxide flakes. *Beilstein J. Nanotechnol.* 10 (1), 71–78. doi:10.3762/bjnano.10.7

Mukhina, M., Danilov, V. V., Orlova, A. O., Fedorov, M. V., Artemyev, M. V., and Baranov, A. V. (2012). Electrically controlled polarized photoluminescence of CdSe/ZnS nanorods embedded in a liquid crystal template. *Nanotechnology* 23 (32), 325201. doi:10.1088/0957-4484/23/32/325201

Müller, J., Sönnichsen, C., von Poschinger, H., von Plessen, G., Klar, T. A., and Feldmann, J. (2002). Electrically controlled light scattering with single metal nanoparticles. *Appl. Phys. Lett.* 81 (1), 171–173. doi:10.1063/1.1491003

Mušević, I., and Škarabot, M. (2008). Self-assembly of nematic colloids. *Soft Matter* 4 (2), 195–199. doi:10.1039/b714250a

Musevic, I., Sōkarabot, M., Tkalec, U., Ravnik, M., and Zōumer, S. (2006). Two-dimensional nematic colloidal crystals self-assembled by topological defects. *Science* 313 (5789), 954–958. doi:10.1126/science.1129660

Myroshnychenko, V., Rodríguez-Fernández, J., Pastoriza-Santos, I., Funston, A. M., Novo, C., Mulvaney, P., et al. (2008). Modelling the optical response of gold nanoparticles. *Chem. Soc. Rev.* 37 (9), 1792–1805. doi:10.1039/b711486a

Nakata, M., Zanchetta, G., Buscaglia, M., Bellini, T., and Clark, N. A. (2008). Liquid crystal alignment on a chiral surface: interfacial interaction with sheared DNA films. *Langmuir* 24 (18), 10390–10394. doi:10.1021/la800639x

Neha, Singh, M., Malik, P., Kumar, S., Malik, P., Singh, A. K., et al. (2023a). Tunable optical, electro-optical and dielectric properties of eco-friendly graphene quantum dots-nematic liquid crystal composites. *Liquid Crystals* 50(13-14), 2345–2359.

Neha, Singh, G., Kumar, S., Malik, P., and Supreet, (2023b). Recent trends and insights into carbon dots dispersed liquid crystal composites. *J. Mol. Liq.* 384, 122225. doi:10.1016/j.molliq.2023.122225

Neto, A. M. F., and Salinas, S. R. (2005). OUP oxford. *Phys. lyotropic Liq. Cryst. phase transitions Struct. Prop.* 62. doi:10.1093/acprof:oso/9780198525509.001.0001

Novoselov, K. S., Geim, A. K., Morozov, S. V., Jiang, D., Zhang, Y., Dubonos, S. V., et al. (2004). Electric field effect in atomically thin carbon films. *science* 306 (5696), 666–669. doi:10.1126/science.1102896

O Dolgov, L., and V Yaroshchuk, O. (2004). Electrooptic properties of liquid crystals filled with silica nanoparticles of different sorts. *Colloid Polym. Sci.* 282, 1403–1408. doi:10.1007/s00396-004-1151-y

Ohzono, T., and Fukuda, J. i. (2012). Zigzag line defects and manipulation of colloids in a nematic liquid crystal in microwrinkle grooves. *Nat. Commun.* 3 (1), 701. doi:10.1038/ncomms1709

Okutan, M., Eren San, S., Basaran, E., and Yakuphanoglu, F. (2005b). Determination of phase transition from nematic to isotropic state in carbon nano-balls' doped nematic liquid crystals by electrical conductivity-dielectric measurements. *Phys. Lett. A* 339 (6), 461–465. doi:10.1016/j.physleta.2005.04.009

Okutan, M., Eren San, S., Köysal, O., and Yakuphanoglu, F. (2005a). Investigation of refractive index dispersion and electrical properties in carbon nano-balls' doped nematic liquid crystals. *Phys. B Condens. Matter* 362 (1-4), 180–186. doi:10.1016/j.physb.2005.02.009

Oldenbourg, R., Wen, X., Meyer, R. B., and Caspar, D. L. D. (1988). Orientational distribution function in nematic tobacco-mosaic-virus liquid crystals measured by x-ray diffraction. *Phys. Rev. Lett.* 61 (16), 1851–1854. doi:10.1103/physrevlett.61.1851

Olmsted, P. D., and Goldbart, P. M. (1992). Isotropic-nematic transition in shear flow: state selection, coexistence, phase transitions, and critical behavior. *Phys. Rev. A* 46 (8), 4966–4993. doi:10.1103/physreva.46.4966

Onsager, L. (1949). The effects of shape on the interaction of colloidal particles. Annals of the New York Academy of Sciences. *Ann. N. Y. Acad. Sci.* 51 (4), 627–659. doi:10.1111/j.1749-6632.1949.tb27296.x

Oswald, P., and Pieranski, P. (2005). CRC press. *Nematic cholesteric Liq. Cryst. concepts Phys. Prop. Illus. by Exp*. doi:10.1201/9780203023013

Ouskova, E., Buchnev, O., Reshetnyak, V., Reznikov, Y., and Kresse, H. (2003). Dielectric relaxation spectroscopy of a nematic liquid crystal doped with ferroelectric Sn 2 P 2 S 6 nanoparticles. *Liq. Cryst.* 30 (10), 1235–1239. doi:10.1080/02678290310001601996

Özgan, Ş., Eskalen, H., and Tapkıranlı, Y. (2018). Thermal and electro-optic properties of graphene oxide-doped hexylcyanobiphenyl liquid crystal. *J. Theor. Appl. Phys.* 12, 169–176. doi:10.1007/s40094-018-0307-y

Pal, K., Sajjadifar, S., Abd Elkodous, M., Alli, Y. A., Gomes, F., Jeevanandam, J., et al. (2019). Soft, self-assembly liquid crystalline nanocomposite for superior switching. *Electron. Mater. Lett.* 15, 84–101. doi:10.1007/s13391-018-0098-y

Pal, K., Zhan, B., Madhu Mohan, M., Schirhagl, R., and Wang, G. (2015). Influence of ZnO nanostructures in liquid crystal interfaces for bistable switching applications. *Appl. Surf. Sci.* 357, 1499–1510. doi:10.1016/j.apsusc.2015.09.229

Pandey, A. S., Dhar, R., Kumar, S., and Dabrowski, R. (2011). Enhancement of the display parameters of 4′-pentyl-4-cyanobiphenyl due to the dispersion of functionalised gold nano particles. *Liq. Cryst.* 38 (1), 115–120. doi:10.1080/02678292.2010.530695

Park, S., Baker, J.O., Himmel, M. E., Parilla, P.A., Johnson, D. K., et al. (2010). Cellulose crystallinity index: measurement techniques and their impact on interpreting cellulase performance. *Biotechnology for biofuels*. 3, 1–10.

Park, S. Y., and Stroud, D. (2004). Splitting of surface plasmon frequencies of metal particles in a nematic liquid crystal. *Appl. Phys. Lett.* 85 (14), 2920–2922. doi:10.1063/1.1800278

Park, S. Y., and Stroud, D. (2005). Surface-enhanced plasmon splitting in a liquid-crystal-coated gold nanoparticle. *Phys. Rev. Lett.* 94 (21), 217401. doi:10.1103/physrevlett.94.217401

Paul, S. N., Dhar, R., Verma, R., Sharma, S., and Dabrowski, R. (2011). Change in dielectric and electro-optical properties of a nematic material (6CHBT) due to the dispersion of BaTiO3 nanoparticles. *Mol. Cryst. Liq. Cryst.* 545 (1), 105. doi:10.1080/15421406.2011.571961

Petrov, A. G. (1999). *The lyotropic state of matter: molecular physics and living matter physics*. Amsterdam, The Netherlands: Gordon and Breach Science Publishers.

Ping, J., Qi, L., Wang, Q., Liu, S., Jiang, Y., Yu, L., et al. (2021). An integrated liquid crystal sensing device assisted by the surfactant-embedded smart hydrogel. *Biosens. Bioelectron.* 187, 113313. doi:10.1016/j.bios.2021.113313

Podoliak, N., Buchnev, O., Herrington, M., Mavrona, E., Kaczmarek, M., Kanaras, A. G., et al. (2014). Elastic constants, viscosity and response time in nematic liquid crystals doped with ferroelectric nanoparticles. *RSC Adv.* 4 (86), 46068–46074. doi:10.1039/c4ra06248e

Poryvai, A., Šmahel, M., Švecová, M., Nemati, A., Shadpour, S., Ulbrich, P., et al. (2022). Chiral, magnetic, and photosensitive liquid crystalline nanocomposites based on multifunctional nanoparticles and achiral liquid crystals. *ACS Nano* 16 (8), 11833–11841. doi:10.1021/acsnano.1c10594

Poulin, P., Stark, H., Lubensky, T. C., and Weitz, D. A. (1997). Novel colloidal interactions in anisotropic fluids. *Science* 275 (5307), 1770–1773. doi:10.1126/science.275.5307.1770

Prakash, J., Choudhary, A., Kumar, A., Mehta, D. S., and Biradar, A. M. (2008). Nonvolatile memory effect based on gold nanoparticles doped ferroelectric liquid crystal. *Appl. Phys. Lett.* 93, 93. doi:10.1063/1.2980037

Prasad, S. K., Kumar, M. V., Shilpa, T., and Yelamaggad, C. V. (2014). Enhancement of electrical conductivity, dielectric anisotropy and director relaxation frequency in composites of gold nanoparticle and a weakly polar nematic liquid crystal. *RSC Adv.* 4 (9), 4453–4462. doi:10.1039/c3ra45761c

Prévôt, M. E., Nemati, A., Cull, T. R., Hegmann, E., and Hegmann, T. (2020). A zero-power optical, ppt- to ppm-level toxic gas and vapor sensor with image, text, and analytical capabilities. *Adv. Mater. Technol.* 5 (5), 2000058. doi:10.1002/admt.202000058

Price, A. D., and Schwartz, D. K. (2008). DNA hybridization-induced reorientation of liquid crystal anchoring at the nematic liquid crystal/aqueous interface. *J. Am. Chem. Soc.* 130 (26), 8188–8194. doi:10.1021/ja0774055

Priscilla, P., Malik, P., Supreet, Kumar, A., Castagna, R., and Singh, G. (2023). Recent advances and future perspectives on nanoparticles-controlled alignment of liquid crystals for displays and other photonic devices. *Critical Reviews in Solid State and Materials Sciences* 48, 57, 92. doi:10.1080/10408436.2022.2027226

Proctor, J. E., Armada, D. M., and Vijayaraghavan, A. (2017). *An introduction to graphene and carbon nanotubes*. Boca Raton, FL: Taylor & Francis Group.

Qi, H., and Hegmann, T. (2006). Formation of periodic stripe patterns in nematic liquid crystals doped with functionalized gold nanoparticles. *J. Mater. Chem.* 16 (43), 4197–4205. doi:10.1039/b611501b

Qi, H., and Hegmann, T. (2011). Liquid crystal–gold nanoparticle composites. *Liq. Cryst. Today* 20 (4), 102–114. doi:10.1080/1358314x.2011.610133

Qi, H., Kinkead, B., Marx, V. M., Zhang, H. R., and Hegmann, T. (2009). Miscibility and alignment effects of mixed monolayer cyanobiphenyl liquid-crystal-capped gold nanoparticles in nematic cyanobiphenyl liquid crystal hosts. *ChemPhysChem* 10 (8), 1211–1218. doi:10.1002/cphc.200800765

Querejeta-Fernández, A., Chauve, G., Methot, M., Bouchard, J., and Kumacheva, E. (2014). Chiral plasmonic films formed by gold nanorods and cellulose nanocrystals. *J. Am. Chem. Soc.* 136 (12), 4788–4793. doi:10.1021/ja501642p

Raina, K. (2013). Nickel nanoparticles doped ferroelectric liquid crystal composites. *Opt. Mater.* 35 (3), 531–535. doi:10.1016/j.optmat.2012.10.014

Reich, S., Thomsen, C., and Maultzsch, J. (2008). John wiley and sons. *Carbon Nanotub. basic concepts Phys. Prop*.

Revol, J.-F., Bradford, H., Giasson, J., Marchessault, R., and Gray, D. (1992). Helicoidal self-ordering of cellulose microfibrils in aqueous suspension. *Int. J. Biol. Macromol.* 14 (3), 170–172. doi:10.1016/s0141-8130(05)80008-x

Reznikov, Y., Buchnev, O., Glushchenko, A., Reshetnyak, V., Tereshchenko, O., and West, J. (2005). Ferroelectric particles-liquid crystal dispersions. *Emerg. Liq. Cryst. Technol.* 5741, 171. doi:10.1117/12.589767

Reznikov, Y., Buchnev, O., Tereshchenko, O., Reshetnyak, V., Glushchenko, A., and West, J. (2003). Ferroelectric nematic suspension. *Appl. Phys. Lett.* 82 (12), 1917–1919. doi:10.1063/1.1560871

Rojas, O. J. (2016) *Cellulose chemistry and properties: fibers, nanocelluloses and advanced materials*, Vol. 271. Springer.

Rudzki, A., Evans, D. R., Cook, G., and Haase, W. (2013). Size dependence of harvested BaTiO 3 nanoparticles on the electro-optic and dielectric properties of ferroelectric liquid crystal nanocolloids. *Appl. Opt.*, 52 (22), E6–E14. doi:10.1364/AO.52.0000E6

Saha, P., and Davis, V. A. (2018). Photonic properties and applications of cellulose nanocrystal films with planar anchoring. *ACS Appl. Nano Mater.* 1 (5), 2175–2183. doi:10.1021/acsanm.8b00233

Saliba, S., Mingotaud, C., Kahn, M. L., and Marty, J. D. (2013). Liquid crystalline thermotropic and lyotropic nanohybrids. *Nanoscale* 5 (15), 6641–6661. doi:10.1039/c3nr01175e

Saraiva, D. V., Remiëns, S. N., Jull, E. I., Vermaire, I. R., and Tran, L. (2024). Flexible, photonic Films of surfactant-functionalized cellulose Nanocrystals for Pressure and humidity sensing. *Small structures* 2400104.

Sasikala, S. P., Lim, J., Kim, I. H., Jung, H. J., Yun, T., Han, T. H., et al. (2018). Graphene oxide liquid crystals: a frontier 2D soft material for graphene-based functional materials. *Chem. Soc. Rev.* 47 (16), 6013–6045. doi:10.1039/c8cs00299a

Scalia, G., Lagerwall, J. P. F., Schymura, S., Haluska, M., Giesselmann, F., and Roth, S. (2007). Carbon nanotubes in liquid crystals as versatile functional materials. *Phys. status solidi (b)* 244 (11), 4212–4217. doi:10.1002/pssb.200776205

Schram, C. J., Beaudoin, S. P., and Taylor, L. S. (2015). Impact of polymer conformation on the crystal growth inhibition of a poorly water-soluble drug in aqueous solution. *Langmuir* 31 (1), 171–179. doi:10.1021/la503644m

Schwartz, J. J., Mendoza, A. M., Wattanatorn, N., Zhao, Y., Nguyen, V. T., Spokoyny, A. M., et al. (2016). Surface dipole control of liquid crystal alignment. *J. Am. Chem. Soc.* 138 (18), 5957–5967. doi:10.1021/jacs.6b02026

Schymura, S., and Scalia, G. (1988). On the effect of carbon nanotubes on properties of liquid crystals. Philosophical Transactions of the Royal Society A: mathematical. *Phys. Eng. Sci.* 2013, 20120261. doi:10.1098/rsta.2012.0261

Shadpour, S., Vanegas, J. P., Nemati, A., and Hegmann, T. (2019). Amplification of chirality by adenosine monophosphate-capped luminescent gold nanoclusters in nematic lyotropic chromonic liquid crystal tactoids. *ACS omega* 4 (1), 1662–1668. doi:10.1021/acsomega.8b03335

Shelestiuk, S. M., Reshetnyak, V. Y., and Sluckin, T. J. (2011). Frederiks transition in ferroelectric liquid-crystal nanosuspensions. *Phys. Rev. E* 83 (4), 041705. doi:10.1103/physreve.83.041705

Shen, T.-Z., Hong, S.-H., and Song, J.-K. (2014). Electro-optical switching of graphene oxide liquid crystals with an extremely large Kerr coefficient. *Nat. Mater.* 13 (4), 394–399. doi:10.1038/nmat3888

Shiraishi, Y., Toshima, N., Maeda, K., Yoshikawa, H., Xu, J., and Kobayashi, S. (2002). Frequency modulation response of a liquid-crystal electro-optic device doped with nanoparticles. *Appl. Phys. Lett.* 81 (15), 2845–2847. doi:10.1063/1.1511282

Shukla, R. K., Chaudhary, A., Bubnov, A., and Raina, K. K. (2018). Multi-walled carbon nanotubes-ferroelectric liquid crystal nanocomposites: effect of cell thickness and dopant concentration on electro-optic and dielectric behaviour. *Liq. Cryst.* 45 (11), 1672–1681. doi:10.1080/02678292.2018.1469170

Shukla, R. K., Raina, K. K., and Haase, W. (2014). Fast switching response and dielectric behaviour of fullerene/ferroelectric liquid crystal nanocolloids. *Liq. Cryst.* 41 (12), 1726–1732. doi:10.1080/02678292.2014.949889

Siepmann, J., and Peppas, N. A. (2012). Modeling of drug release from delivery systems based on hydroxypropyl methylcellulose (HPMC). *Adv. drug Deliv. Rev.* 64, 163–174. doi:10.1016/j.addr.2012.09.028

Singh, D., Bahadur Singh, U., Bhushan Pandey, M., Dabrowski, R., and Dhar, R. (2018a). Improvement of orientational order and display parameters of liquid crystalline material dispersed with single-wall carbon nanotubes. *Mater. Lett.* 216, 5–7. doi:10.1016/j.matlet.2017.12.099

Singh, D., Singh, U., Pandey, M., Dabrowski, R., and Dhar, R. (2018b). Enhancement in electro-optical parameters of nematic liquid crystalline material with SWCNTs. *Opt. Mater.* 84, 16–21. doi:10.1016/j.optmat.2018.06.045

Singh, D., Singh, U. B., Dhar, R., Dabrowski, R., and Pandey, M. B. (2021). Enhancement of electro-optical and dielectric parameters of a room temperature nematic liquid crystalline material by dispersing multi-walled carbon nanotubes. *Liq. Cryst.* 48 (3), 307–312. doi:10.1080/02678292.2020.1777591

Singh, U., Dhar, R., Dabrowski, R., and Pandey, M. (2014). Enhanced electro-optical properties of a nematic liquid crystals in presence of BaTiO3 nanoparticles. *Liq. Cryst.* 41 (7), 953–959. doi:10.1080/02678292.2014.894209

Singh, U., Dhar, R., Dabrowski, R., and Pandey, M. B. (2013). Influence of low concentration silver nanoparticles on the electrical and electro-optical parameters of nematic liquid crystals. *Liq. Cryst.* 40 (6), 774–782. doi:10.1080/02678292.2013.783136

Sivakumar, S., Wark, K. L., Gupta, J. K., Abbott, N. L., and Caruso, F. (2009). Liquid crystal emulsions as the basis of biological sensors for the optical detection of bacteria and viruses. *Adv. Funct. Mater.* 19 (14), 2260–2265. doi:10.1002/adfm.200900399

Smaisim, G. F., Mohammed, K. J., Hadrawi, S. K., Koten, H., and Kianfar, E. (2023). Properties and application of nanostructure in liquid crystals: review. *BioNanoScience* 13 (2), 819–839. doi:10.1007/s12668-023-01082-5

Smalyukh, I. I. (2018). Liquid crystal colloids. *Annu. Rev. Condens. Matter Phys.* 9, 207–226. doi:10.1146/annurev-conmatphys-033117-054102

Song, W., Kinloch, I. A., and Windle, A. H. (2003). Nematic liquid crystallinity of multiwall carbon nanotubes. *Science* 302 (5649), 1363. doi:10.1126/science.1089764

Song, W., and Windle, A. H. (2005). Isotropic– nematic phase transition of dispersions of multiwall carbon nanotubes. *Macromolecules* 38 (14), 6181–6188. doi:10.1021/ma047691u

Song, W., and Windle, A. H. (2008). Size-dependence and elasticity of liquid-crystalline multiwalled carbon nanotubes. *Adv. Mater.* 20 (16), 3149–3154. doi:10.1002/adma.200702972

Stankovich, S., Dikin, D. A., Dommett, G. H. B., Kohlhaas, K. M., Zimney, E. J., Stach, E. A., et al. (2006). Graphene-based composite materials. *Nature* 442(7100). 282–286. doi:10.1038/nature04969

Stannarius, R. (2009). More than display fillings. *Nat. Mater.* 8 (8), 617–618. doi:10.1038/nmat2503

Stark, H. (2001). Physics of colloidal dispersions in nematic liquid crystals. *Phys. Rep.* 351 (6), 387–474. doi:10.1016/s0370-1573(00)00144-7

Strzelecka, T. E., Davidson, M. W., and Rill, R. L. (1988). Multiple liquid crystal phases of DNA at high concentrations. *Nature* 331 (6155), 457–460. doi:10.1038/331457a0

Su, K.-H., Wei, Q. H., Zhang, X., Mock, J. J., Smith, D. R., and Schultz, S. (2003). Interparticle coupling effects on plasmon resonances of nanogold particles. *Nano Lett.* 3 (8), 1087–1090. doi:10.1021/nl034197f

Sun, C., Zhang, S., Ren, Y., Zhang, J., Shen, J., Qin, S., et al. (2022). Force-induced synergetic pigmentary and structural color change of liquid crystalline elastomer with nanoparticle-enhanced mechanosensitivity. *Adv. Sci. (Weinh).* 9 (36), 2205325. doi:10.1002/advs.202205325

Tan, H., Yang, S., Shen, G., Yu, R., and Wu, Z. (2010). Signal-enhanced liquid-crystal DNA biosensors based on enzymatic metal deposition. *Angew. Chem. Int. Ed.* 49 (46), 8608–8611. doi:10.1002/anie.201004272

Tripathi, A. K., Singh, M. K., Mathpal, M. C., Mishra, S. K., and Agarwal, A. (2013a). Study of structural transformation in TiO2 nanoparticles and its optical properties. *J. Alloys Compd.* 549, 114–120. doi:10.1016/j.jallcom.2012.09.012

Tripathi, P., Mishra, M., Kumar, S., Dabrowski, R., and Dhar, R. (2018). Dependence of physical parameters on the size of silver nano particles forming composites with a nematic liquid crystalline material. *J. Mol. Liq.* 268, 403–409. doi:10.1016/j.molliq.2018.07.046

Tripathi, P., Singh, D., Yadav, T., Singh, V., Srivastava, A., and Negi, Y. (2023). Enhancement of birefringence for liquid crystal with the doping of ferric oxide nanoparticles. *Opt. Mater.* 135, 113298. doi:10.1016/j.optmat.2022.113298

Tripathi, P. K., Misra, A. K., Manohar, S., Gupta, S. K., and Manohar, R. (2013b). Improved dielectric and electro-optical parameters of ZnO nano-particle (8% Cu2+) doped nematic liquid crystal. *J. Mol. Struct.* 1035, 371–377. doi:10.1016/j.molstruc.2012.10.052

Tyagi, M., Chandran, A., Joshi, T., Prakash, J., Agrawal, V. V., and Biradar, A. M. (2014). Self assembled monolayer based liquid crystal biosensor for free cholesterol detection. *Appl. Phys. Lett.* 104, 154104. doi:10.1063/1.4871704

Varshney, D., Prakash, J., and Singh, G. (2023b). Indium tin oxide nanoparticles induced molecular rearrangement in nematic liquid crystal material. *J. Mol. Liq.* 387, 122578. doi:10.1016/j.molliq.2023.122578

Varshney, D., Prakash, J., and Singh, G. (2023c). Indium tin oxide nanoparticles induced tunable dual alignment in nematic liquid crystal. *J. Mol. Liq.* 374, 121264. doi:10.1016/j.molliq.2023.121264

Varshney, D., Yadav, K., Prakash, J., Meena, H., and Singh, G. (2023a). Tunable dielectric and memory features of ferroelectric layered perovskite Bi4Ti3O12 nanoparticles doped nematic liquid crystal composite. *J. Mol. Liq.* 369, 120820. doi:10.1016/j.molliq.2022.120820

Verma, H., Lal, A., Singh, P. K., Pandey, M. B., Dabrowski, R., and Dhar, R. (2024). Silver nanoparticles induced enhanced stability, dielectric anisotropy, and electro-optical parameters of a nematic liquid crystalline material 4-(trans-4-n-hexylcyclohexyl) isothiocyanatobenzene. *J. Mol. Liq.* 400, 124503. doi:10.1016/j.molliq.2024.124503

Vimal, T., Kumar Gupta, S., Katiyar, R., Srivastava, A., Czerwinski, M., Krup, K., et al. (2017). Effect of metallic silver nanoparticles on the alignment and relaxation behaviour of liquid crystalline material in smectic C* phase. *J. Appl. Phys.* 122, 122. doi:10.1063/1.5003247

Vovk, V., Koval'chuk, A., and Lebovka, N. (2012). Impact of homeotropic and planar alignment of liquid crystalline medium on the structure and dielectric properties of modified fullerene mC60+ E25M mixtures. *Liq. Cryst.* 39 (1), 77–86. doi:10.1080/02678292.2011.611902

Wang, H., Xu, T., Fu, Y., Wang, Z., Leeson, M. S., Jiang, J., et al. (2022d). Liquid crystal biosensors: principles, structure and applications. *Biosensors* 12 (8), 639. doi:10.3390/bios12080639

Wang, L., Urbas, A. M., and Li, Q. (2020). Nature-inspired emerging chiral liquid crystal nanostructures: from molecular self-assembly to DNA mesophase and nanocolloids. *Adv. Mater.* 32 (41), 1801335. doi:10.1002/adma.201801335

Wang, X., Hu, W., Chen, G., Chen, H., Huang, R., Ren, Y., et al. (2022a). TiO_2 doped polymer dispersed and stabilised liquid crystal smart film with high contrast ratio, low driving voltage and short response time. *Liq. Cryst.* 49 (12), 1623–1632. doi:10.1080/02678292.2022.2048912

Wang, X., Wang, H., Sun, Y., Liu, Z., and Wang, N. (2024). Liquid crystal biosensor based on AuNPs signal amplification for detection of human chorionic gonadotropin. *Talanta* 266, 125025. doi:10.1016/j.talanta.2023.125025

Wang, Y., Liu, J., and Yang, S. (2022b). Multi-functional liquid crystal elastomer composites. *Appl. Phys. Rev.* 9, 9. doi:10.1063/5.0075471

Wang, Z., Liu, Y., Wang, H., Wang, S., Liu, K., Xu, T., et al. (2022c). Ultra-sensitive DNAzyme-based optofluidic biosensor with liquid crystal-Au nanoparticle hybrid amplification for molecular detection. *Sensors Actuators B Chem.* 359, 131608. doi:10.1016/j.snb.2022.131608

Whitesides, G. M., and Grzybowski, B. (2002). Self-assembly at all scales. *Science* 295 (5564), 2418–2421. doi:10.1126/science.1070821

Williams, C. A., Parker, R. M., Kyriacou, A., Murace, M., and Vignolini, S. (2024). Inkjet printed photonic cellulose nanocrystal patterns. *Adv. Mater.* 36 (1), 2307563. doi:10.1002/adma.202307563

Williams, Y., Chen, K., Park, J. H., Khoo, I. C., Lewis, B., and Mallouk, T. E. (2005). Electro-optical and nonlinear optical properties of semiconductor nanorod doped liquid crystals. *Liq. Cryst. IX* 5936, 593613. doi:10.1117/12.617730

Woltman, S. J., Jay, G. D., and Crawford, G. P. (2007). Liquid-crystal materials find a new order in biomedical applications. *Nat. Mater.* 6 (12), 929–938. doi:10.1038/nmat2010

Wu, P.-C., and Lee, W. (2013). Phase and dielectric behaviors of a polymorphic liquid crystal doped with graphene nanoplatelets. *Appl. Phys. Lett.* 102, 102. doi:10.1063/1.4802839

Xu, Z., and Gao, C. (2011a). Graphene chiral liquid crystals and macroscopic assembled fibres. *Nat. Commun.* 2 (1), 571. doi:10.1038/ncomms1583

Xu, Z., and Gao, C. (2011b). Aqueous liquid crystals of graphene oxide. *ACS nano* 5 (4), 2908–2915. doi:10.1021/nn200069w

Yada, M., Yamamoto, J., and Yokoyama, H. (2004). Direct observation of anisotropic interparticle forces in nematic colloids with optical tweezers. *Phys. Rev. Lett.* 92 (18), 185501. doi:10.1103/physrevlett.92.185501

Yadav, G., Kumar, M., Srivastava, A., and Manohar, R. (2019). SiO2 nanoparticles doped nematic liquid crystal system: an experimental investigation on optical and dielectric properties. *Chin. J. Phys.* 57, 82–89. doi:10.1016/j.cjph.2018.12.008

Yadav, S., Malik, P., Khushboo, and Jayoti, D. (2020). Electro-optical, dielectric and optical properties of graphene oxide dispersed nematic liquid crystal composites. *Liq. Cryst.* 47 (7), 984–993. doi:10.1080/02678292.2019.1695969

Yaduvanshi, P., Kumar, S., and Dhar, R. (2015). Effects of copper nanoparticles on the thermodynamic, electrical and optical properties of a disc-shaped liquid crystalline material showing columnar phase. *Phase Transitions* 88 (5), 489–502. doi:10.1080/01411594.2014.984710

Yakemseva, M., Dierking, I., Kapernaum, N., Usoltseva, N., and Giesselmann, F. (2014). Dispersions of multi-wall carbon nanotubes in ferroelectric liquid crystals. *The European Physical Journal E.* 37, 1–7.

Yakovkin, I., and Reshetnyak, V. (2023). Controlling plasmon resonance of gold and silver nanoparticle arrays with help of liquid crystal. *Photonics* 10, 1088. doi:10.3390/photonics10101088

Yang, S., Liu, Y., Tan, H., Wu, C., Wu, Z., Shen, G., et al. (2012). Gold nanoparticle based signal enhancement liquid crystal biosensors for DNA hybridization assays. *Chem. Commun.* 48 (23), 2861–2863. doi:10.1039/c2cc17861c

Ye, W., Yuan, R., Dai, Y., Gao, L., Pang, Z., Zhu, J., et al. (2017). Improvement of image sticking in liquid crystal display doped with γ-Fe2O3 nanoparticles. *Nanomaterials* 8 (1), 5. doi:10.3390/nano8010005

Yoshida, H., Tanaka, Y., Kawamoto, K., Kubo, H., Tsuda, T., Fujii, A., et al. (2009). Nanoparticle-stabilized cholesteric blue phases. *Appl. Phys. express* 2 (12), 121501. doi:10.1143/apex.2.121501

Yoshikawa, H., Maeda, K., Shiraishi, Y., Xu, J., Shiraki, H., and Toshima, N. (2002). Frequency modulation response of a tunable birefringent mode nematic liquid crystal electrooptic device fabricated by doping nanoparticles of Pd covered with liquid-crystal molecules. *Jpn. J. Appl. Phys.*, 41 (11B), L1315. doi:10.1143/JJAP.41.L1315

Yu, L., Shearer, C., and Shapter, J. (2016). Recent development of carbon nanotube transparent conductive films. *Chem. Rev.* 116 (22), 13413–13453. doi:10.1021/acs.chemrev.6b00179

Zhang, R., Du, W., Shao, F., Li, S., Kuai, Y., Cao, Z., et al. (2023b). Voltage, thermal and magnetic field fiber sensors based on magnetic nanoparticles-doped photonic liquid crystal fibers. *Opt. Express* 31 (16), 25372–25384. doi:10.1364/oe.492364

Zhang, S., Majewski, P. W., Keskar, G., Pfefferle, L. D., and Osuji, C. O. (2011). Lyotropic self-assembly of high-aspect-ratio semiconductor nanowires of single-crystal ZnO. *Langmuir* 27 (18), 11616–11621. doi:10.1021/la200703u

Zhang, Y., Liu, Q., Mundoor, H., Yuan, Y., and Smalyukh, I. I. (2015). Metal nanoparticle dispersion, alignment, and assembly in nematic liquid crystals for applications in switchable plasmonic color filters and E-polarizers. *ACS Nano* 9 (3), 3097–3108. doi:10.1021/nn5074644

Zhang, Z., Chen, Z., Wang, Y., Zhao, Y., and Shang, L. (2022). Cholesteric cellulose liquid crystals with multifunctional structural colors. *Adv. Funct. Mater.* 32 (12), 2107242. doi:10.1002/adfm.202107242

Zhang, Z., Yang, X., Zhao, Y., Ye, F., and Shang, L. (2023a). Liquid crystal materials for biomedical applications. *Adv. Mater.* 35 (36), 2300220. doi:10.1002/adma.202300220

Zhao, Y., Li, J., Yu, Y., Zhao, Y., Guo, Z., Yao, R., et al. (2022). Electro-optical characteristics of polymer dispersed liquid crystal doped with MgO nanoparticles. *Molecules* 27 (21), 7265. doi:10.3390/molecules27217265